

## The formation of carbon filaments upon decomposition of hydrocarbons catalysed by iron subgroup metals and their alloys

To cite this article: Vladimir V Chesnokov and Roman A Buyanov 2000 *Russ. Chem. Rev.* **69** 623

View the [article online](#) for updates and enhancements.

### You may also like

- [Bacterial filamentation accelerates colonization of adhesive spots embedded in biopassive surfaces](#)  
Jens Möller, Philippe Emge, Ima Avalos Vizcarra et al.
- [Kinetics of filamentous phage assembly](#)  
Martin Ploss and Andreas Kuhn
- [Effects of sensilla morphology on mechanosensory sensitivity in the crayfish](#)  
Swapnil Pravin, DeForest Mellon, Edward J Berger et al.

# The formation of carbon filaments upon decomposition of hydrocarbons catalysed by iron subgroup metals and their alloys

V V Chesnokov, R A Buyanov

## Contents

I. Introduction	623
II. The carbide cycle mechanism of carbon formation	623
III. Regularities in the formation of carbon of different morphological types on iron subgroup metals	626
IV. Conclusion	636

**Abstract.** The structure of filamentous carbon formed upon catalytic decomposition of hydrocarbons on iron subgroup metals and their alloys is considered. The regularities of the deposition of carbon on these metals are generalised. The carbide cycle mechanism of carbon formation is considered in detail. The growth models of some morphological modifications of filamentous carbon are discussed. The bibliography includes 151 references.

## I. Introduction

Deactivation of catalysts may be determined by a number of factors,<sup>1</sup> one of which is carbonisation (coking) of catalysts in the processing of hydrocarbons. The development of an efficient method for combating this phenomenon would allow substantial extension of the lifetime of catalysts; therefore, the interest of investigators in the mechanisms of catalytic formation of carbon has not decreased for many decades. This interest is also due to the fact that in a number of cases, the carbonised mineral phases (metals, oxides, and others) and carbon itself can be regarded as carbon-mineral and carbon composite materials possessing special properties.

The formation of filamentous carbon upon decomposition of hydrocarbons on iron subgroup metals and their alloys is one of the most exotic (from the viewpoint of its mechanism) and practically important processes. The properties of carbon graphite deposits on catalysts are mainly determined by their morphological and crystallographic features. The main task in the development of technologies for the preparation of a broad spectrum of such composites should be the elaboration of a scientifically substantiated procedure of process control. To the end, it is necessary to know the mechanisms underlying all its stages.

## II. The carbide cycle mechanism of carbon formation

### 1. Decomposition of hydrocarbons on metallic iron

Various suggestions on the possible role of carbides as intermediates in the formation of carbon deposits were put forward in early

studies generalised by Storch *et al.*<sup>2</sup> in their monograph nearly five decades ago. It has been noted, in particular, that the hypothesis according to which carbides are intermediates in the formation of free carbon is attractive but stands in need of evidence.

Kagan *et al.*<sup>3</sup> considered carbonisation of an iron catalyst to be the result of two independent reactions



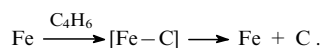
However, a later study proved<sup>4</sup> that the important parts of the process of carbon formation in the decomposition of hydrocarbons on iron are the steps of carbide formation and decomposition.

The proposed carbide mechanism of carbon formation could be confirmed by the establishment of a common limiting step and a common intermediate in the formation of a carbide and carbon. To this end, the activation energies of carbon and iron carbide formation<sup>5,6</sup> were measured in the experiments on carbonisation of iron in the butadiene decomposition. The formation of the carbide in the temperature range 573–723 K is virtually unaccompanied by its decomposition and liberation of carbon. The formation of iron carbide  $\text{Fe}_3\text{C}$  is a topochemical reaction, *i.e.*, it occurs through formation and growth of nuclei of the carbide phase. An integral kinetic curve of the reaction is S-shaped; therefore, an approximate formula<sup>7</sup> is used to determine the specific rate of carbidisation

$$W = 2 \frac{W_{\max}}{\pi S},$$

where  $W_{\max}$  is the maximum observed rate of carbidisation,  $S$  is the specific surface of a sample. The activation energy was determined from the  $W_{\max}$  values at different temperatures.

In the range of temperatures 808–874 K, the activation energy of carbide decomposition ( $197 \text{ kJ mol}^{-1}$ ) is substantially higher than that of its formation ( $88 \text{ kJ mol}^{-1}$ ). For this reason, the ratio between the rates of these reactions changes with temperature. Above 1023 K, the rate of iron carbide decomposition exceeds the rate of its formation, and the carbide phase is not formed. Investigations into the kinetics of carbon formation on iron showed that the activation energy of carbon formation at 1023–1027 K amounts to  $96 \text{ kJ mol}^{-1}$  and becomes close to that of carbide formation. Obviously, the common limiting step of both reactions is the formation of an intermediate, surface carbide-like compound of the type  $[\text{Fe}-\text{C}]$ . This makes it possible to represent the mechanism of formation of carbon deposits on iron with the following scheme:



V V Chesnokov, R A Buyanov G K Boreskov Institute of Catalysis, Siberian Branch of the Russian Academy of Sciences, Prosp. Akad. Lavrent'eva 5, 630090 Novosibirsk, Russian Federation.  
Fax (7-383) 234 37 66. Tel. (7-383) 234 45 53.  
E-mail: buyanov@catalysis.nsk.su (R A Buyanov)

Received 28 February 2000

*Uspekhi Khimii* 69 (7) 675–692 (2000); translated by V D Gorokhov

In our studies, this mechanism has been called the carbide cycle mechanism.<sup>4–6,8–17</sup> The reactions proceed in an open flow system from which the gaseous decomposition products are removed; therefore, the thermodynamic restrictions here are of minor significance.

The carbide cycle mechanism includes two basic steps:<sup>5</sup> the ‘chemical’ step in which the catalytic decomposition of hydrocarbons occurs on the surface of a metal particle with the formation of carbon atoms whose concentration increases to definite limiting values, and the ‘physical’ step in which the crystallisation centres (nuclei) of the graphite phase are formed on definite faces of a metal particle. In this step, migration (diffusion in the bulk of the metal particle) of carbon atoms towards these centres and growth of a definite variety of graphite particles, predominantly in the form of filaments begin.

Despite the fact that the formation of carbon comprises two steps, the mechanism, on the whole, was called the mechanism of the carbide cycle since the carbon atoms involved in the graphite formation ‘originate’ from intermediate carbide compounds.

The character of carbon deposits is determined by the properties of metal catalyst particles, the nature of a hydrocarbon, as well as by the distinctive features of crystallisation centres and mass-transfer of carbon atoms.

The mechanism of the carbide cycle considered above in the example of the model system  $\text{Fe} + \text{C}_4\text{H}_6$  can also be extended to the decomposition of other hydrocarbons. Naturally, the activation energies of formation of carbon deposits from different hydrocarbons differ substantially: *e.g.*, for methane, butane, propylene, isobutylene and butadiene they are<sup>6,18</sup> 209, 184, 146, 138 and 96  $\text{kJ mol}^{-1}$ , respectively. The relationship between the activation energies ( $E_a$ ) and enthalpies ( $\Delta H$ ) of the iron carbide formation from different hydrocarbons (Fig. 1) is described by the Brønsted–Polanyi equation.

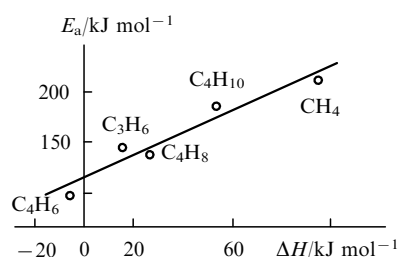
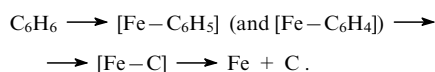


**Figure 1.** Dependence of the activation energy of carbon formation on the enthalpy of iron carbide formation in the decomposition of various hydrocarbons.

The formation of carbon from aromatic hydrocarbons can also occur by the carbide cycle mechanism. This was demonstrated in the example of benzene decomposition on metallic iron.<sup>19</sup> At temperatures above 773 K, the catalyst in the steady state is in the form of metal, whereas below this temperature the metallic iron passes to the carbide. The formation of carbon from benzene on metallic iron in the temperature range 773–998 K can be described by the scheme



At temperatures above  $\sim 898$  K, the limiting step is the dissociative adsorption of benzene accompanied by the formation of  $\text{C}_6\text{H}_5$  or  $\text{C}_6\text{H}_4$  species,<sup>20–22</sup> while below this temperature the reaction is limited by the scission of the benzene ring with the formation of intermediate carbide-like compounds.

## 2. The role of topochemical processes in the mass-transfer of carbon in the carbide cycle mechanism

Studies of the carbon phase formation on metallic iron suggest the elucidation of not only the mechanism of decomposition of hydrocarbons with liberation of carbon atoms, but also of the mode of generation and formation of a new phase from these atoms. The theory of solid-phase reactions<sup>23</sup> and the theory of crystallisation<sup>24</sup> are based on the assumption that the initial formation of nuclei of a new phase is often the limiting step of these processes. Under the conditions of topochemical process, the nuclei are formed on the active centres the role of which can be played by surface defects, associates, clusters, sites of the exit of dislocations onto the surface of crystals, *etc.*

In the decomposition of hydrocarbons accompanied by the formation of intermediate carbide-like compounds, carbon atoms are liberated which diffuse into the bulk of the metal and form there a solid solution.<sup>13</sup> The question arises of how the nuclei of the new phase (graphite) are formed and how does the transport of carbon to these nuclei occur.

In accordance with the carbide cycle mechanism,<sup>4–6,10–18,25</sup> the subsurface layer of the metal becomes supersaturated (by over two orders of magnitude) with the carbon liberated in the decomposition of intermediate carbide compounds. Indeed, the decomposition of intermediate carbide compounds forms a mixture of carbon and the metal in which the C:Fe ratio appears to correspond to the composition  $\text{Fe}_3\text{C}$  ( $\sim 6$  mass % – 7 mass % of carbon), whereas the saturated solution of carbon in iron contains not more than 0.025 mass % of carbon.<sup>26</sup> The concentration of carbon is averaged over the bulk of the metal, and this results in the appearance of a graphite nucleus at one of the sites of the metal particle surface. The growth of the graphite phase occurs by virtue of excess carbon in the supersaturated solution. High gradients of carbon concentration appear between the surface site where decomposition of hydrocarbons takes place and the site where the graphite phase is formed. The presence of such a gradient ensures the diffusive transport of carbon atoms through the bulk of a metal particle.

The appearance of a concentration gradient in a solution of carbon in the metal is explained by the specific features of carbon formation through the carbide cycle mechanism and by the difficulties of graphite nuclei formation.

The above considerations make it possible to present a general scheme of all the steps of the graphite phase formation. The activation energies of deposition of carbon formed upon decomposition of acetylene on  $\alpha$ -iron ( $E_c$ ) and diffusion of carbon through the  $\alpha$ -iron phase ( $E_d$ ) are close,<sup>27</sup> their values are within the range 67–80  $\text{kJ mol}^{-1}$ . This is only possible provided the activation energy of decomposition of hydrocarbons by the carbide cycle mechanism ( $E'$ ) is smaller than  $E_d$ . In this case, the growth of the carbon phase is limited by the step of diffusive transfer of carbon, which predetermines the apparent equality  $E_c \simeq E_d$ . However, the activation energy of the decomposition of a number of more stable hydrocarbons by the carbide cycle mechanism may be rather high and  $E' > E_d$ ; in this case it is not the carbon diffusion but rather the formation of intermediate compound  $[\text{Fe}-\text{C}]$ , *i.e.*, decomposition of hydrocarbons, that becomes the limiting step. Then the values of  $E'$  and  $E_c$  coincide. Thus, the diffusion of carbon in the metal from the site of its liberation towards the nucleus or the graphite phase on which it condenses is an important step in the catalytic process of carbon deposition on metals.<sup>13</sup> Deposition of carbon on iron subgroup metals occurs at increased temperatures when carbides of these metals are not formed (for Fe, Ni and Co, these temperatures amount to 1023, 673 and 573 K, respectively).

Relevant experiments have shown<sup>28</sup> that the formation of graphite nuclei is a more energy-consuming process than the carbide phase formation. This may be explained by the fact that

carbon is formed by the carbide cycle mechanisms through an intermediate surface carbide compound which is transformed into carbide after saturation with carbon from its solid solution in the metal.<sup>13</sup> Under definite conditions, the deposition of carbon can begin with the formation of a thermodynamically unstable metastable carbide phase.<sup>29–32</sup> The carbide formation accompanied by the liberation of elementary carbon was observed, in particular, in CO disproportionation on iron.<sup>7</sup> In this case, the accumulation of carbon in the carbide phase may be regarded as only an intermediate step in the formation of graphite nuclei. Owing to this step, the concentration of carbon in the metal bulk may be considerably higher than merely in the saturated solution of carbon in the metal.

### 3. The formation of carbon on iron carbide

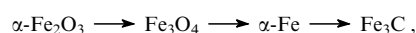
As noted above, under definite conditions a metal catalyst undergoes some changes under the action of the reaction medium and can exist in the form of a metastable carbide in the steady state. For this reason, irrespective of whether the metal or the carbide is the active origin of the process of carbon formation, one can say that carbon will be formed by the carbide cycle mechanism.

Accumulation of carbide-like compounds leads first to the appearance of the Fe<sub>3</sub>C phase nuclei and then to the complete phase transformation of the metal into the carbide. The carbide mechanism of the formation of carbon deposits on Fe<sub>3</sub>C is preserved in any case; however, the features of its implementation are determined by the chemical nature of the active phase.

The chemical nature of the active phase is primarily manifested in the step of decomposition of an intermediate carbide-like compound. The limiting step of the formation of carbon deposits on the metal is the formation of a carbide-like compound, whereas its decomposition and aggregation of the liberated carbon atoms occur rather quickly. The limiting step of carbon formation on the carbide is the liberation of carbon atoms from the carbide, the carbide passing to a transient state with a disturbed stoichiometry. The disturbed stoichiometry of the surface carbide is recovered upon hydrocarbon decomposition. As the bulk of a catalyst contains a considerable amount of carbon, the diffusive transfer of carbon atoms through the carbide bulk virtually does not take place, while their surface migration is negligible. In this case, the carbon phase is formed as islets or a continuous film shielding the catalyst's surface.

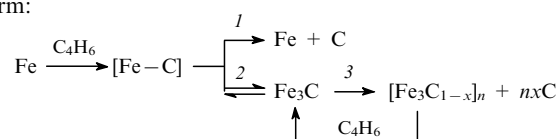
The rate of carbide decomposition increases with temperature. Direct measurements of the initial rate of Fe<sub>3</sub>C decomposition were performed using a high-temperature X-ray chamber.<sup>6, 12</sup>

It was established that  $\alpha$ -Fe<sub>2</sub>O<sub>3</sub> undergoes various transformations under the action of the reaction medium (buta-1,3-diene diluted with helium at the molar ratio 1 : 10)



which occur over 10 min; after this the composition of the catalyst corresponds to iron carbide and remains unchanged with time. The contents of  $\alpha$ -Fe and Fe<sub>3</sub>C in a sample were estimated from the heights of the corresponding peaks (110) and (210) on the diffractograms. In an inert medium, iron carbide decomposes into carbon and a solid solution of carbon in  $\alpha$ -Fe (ferrite). The initial rate of Fe<sub>3</sub>C decomposition coincided with the rate of carbon formation in the presence of the carbide phase.<sup>6</sup> This fact confirms that the formation of carbon deposits is limited by the step of carbon liberation from iron carbide. As a result, iron carbide is depleted in carbon to give a non-stoichiometric carbide with which a hydrocarbon interacts. The carbon atoms formed during decomposition of hydrocarbon by the carbide mechanism are again involved in finishing the 'build-up' of the carbide. X-Ray structural studies showed that the interplanar distances in the carbide correspond to the standard values. Consequently, in the course of reaction the system contains stoichiometric carbide Fe<sub>3</sub>C, while the slow step is the liberation of carbon from it.

A detailed scheme of the catalytic process of formation of carbon deposits by the carbide cycle mechanism has the following form:



where [Fe–C] is the carbide-like intermediate compound, [Fe<sub>3</sub>C<sub>1–x</sub>]<sub>n</sub> is the intermediate surface carbide with disturbed stoichiometry,  $nx = 1$ .

Depending on the conditions, either the carbide phase or the metal phase can be stable; although, naturally, only one phase exists in the steady state. The reaction route 1 corresponds to the formation of carbon from hydrocarbons on a metal without formation of the carbide phase. Reaction 2 describes the phase chemical transformations occurring under the action of the reaction medium. Reaction 3 is related to the liberation of carbon and the subsurface non-stoichiometric carbide which can be saturated with carbon under the action of gaseous hydrocarbons.

### 4. Specific features of the carbide cycle mechanism in the formation of carbon on nickel

The above-cited scheme of the carbide cycle describes the processes occurring on nickel, cobalt and a number of other metals. Naturally, individual features of each metal catalyst are manifested in individual steps of the formation of carbon deposits, though this takes place within the limits of the regularities described.

Let us consider, for example, the features of formation of carbon deposits from butadiene on nickel.<sup>6, 15</sup>

Using a high-temperature X-ray chamber, it was shown that in the hydrocarbon medium, nickel carbide is formed at temperatures below 623 K. In this case, deposition of carbon proceeds very slowly and does not change the kinetics of carbide formation, which was therefore studied in the temperature range 548–623 K, while the kinetics of carbon formation was studied at 773–923 K. The former reaction is of first order with respect to butadiene and is characterised by an activation energy of 96 kJ mol<sup>–1</sup>, while the latter is zero order and has an activation energy of 134 kJ mol<sup>–1</sup>.

These distinctions indicate that the reactions of carbide formation and carbon depositions on nickel have different limit-

**Table 1.** Coefficients of carbon diffusion through iron subgroup metals and their temperature dependences.

T/K	Diffusion coefficient		Temperature dependence <sup>a</sup>	
	D/cm <sup>2</sup> s <sup>–1</sup>	Ref.	D = D <sub>0</sub> exp(–E <sub>a</sub> /RT)	Ref.
<b>Iron</b>				
773	2 × 10 <sup>–8</sup>	41	D = 3.9 × 10 <sup>–3</sup> exp(–80.3/RT)	43
	1 × 10 <sup>–8</sup>	43	D = 8 × 10 <sup>–3</sup> exp(–83/RT)	26
	2 × 10 <sup>–8</sup>	26		
873	1 × 10 <sup>–7</sup>	41		
	5 × 10 <sup>–8</sup>	43		
	8 × 10 <sup>–7</sup>	26		
<b>Cobalt</b>				
773	3 × 10 <sup>–11</sup>	44	D = 0.21 exp(–147/RT)	44
873	5.74 × 10 <sup>–10</sup>	44		
<b>Nickel</b>				
773	8 × 10 <sup>–11</sup>	41	D = 0.1 exp(–138/RT)	41
	2.5 × 10 <sup>–11</sup>	42	D = 2.48 exp(–168/RT)	42
873	8 × 10 <sup>–10</sup>	41		
	2.5 × 10 <sup>–10</sup>	42		

<sup>a</sup> Activation energy E<sub>a</sub> is expressed in kJ mol<sup>–1</sup>.

ing steps. The value of  $E_a$  for the second reaction is  $134 \text{ kJ mol}^{-1}$ , which corresponds to the activation energy of carbon diffusion through this metal.<sup>27,33–39</sup> Consequently, it may be presumed that the limiting step of carbon formation on metallic nickel is its diffusion through nickel to the nuclei and the graphite phase which is being formed. Thus, the limiting steps of the processes of formation of carbon deposits on iron and nickel are different. This is explained by the fact that the coefficient of carbon diffusion in  $\alpha$ -Fe is nearly three orders of magnitude larger than that in nickel (Table 1).<sup>40–44</sup>

At temperatures below 623 K, the formation of  $\text{Ni}_3\text{C}$  carbide occurs considerably faster than its decomposition; in this temperature range, carbon is formed on nickel carbide.

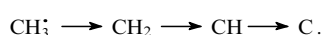
Substitution of benzene or hexane for butadiene does not affect the rate of carbon formation. This may indicate that the formation of carbon from the above-mentioned hydrocarbons on nickel is limited by the same step, *i.e.*, the diffusion of carbon atoms through the bulk of the metal.

### 5. Regularities of carbon formation from methane on nickel

The results of studies of the nature of the active phase of  $\text{Ni/SiO}_2$  catalysts in the reforming of methane by carbon dioxide confirmed the important role of the surface layers of nickel carbide in both implementation of the major transformation and formation of carbon.<sup>45</sup> The reaction proceeds on the surface layer which is formed in the beginning of the process and which is close in its composition to nickel carbide. The adsorbed forms of carbon resulting from the activation of methane on the nickel surface are in equilibrium with methane in the gas phase. They can be irreversibly transformed to CO by reacting with adsorbed oxygen (in different forms), which results from the activation of carbon dioxide. A portion of carbon in the amount equivalent to its content in the subsurface carbide layer is rapidly dissolved in the bulk of nickel. This carbon diffuses into the bulk of the metal and is involved in the formation of carbon deposits.

Owing to high thermodynamic stability of methane, its behaviour in the process of nickel carbonisation is different from that of other hydrocarbons.

Chemisorption and subsequent decomposition of methane on the surface of nickel single crystals were studied by high-resolution spectroscopy of characteristic electron energy losses and by Auger spectroscopy.<sup>46–55</sup> It was established that at lower temperatures, methane is chemisorbed in the dissociative mode with formation of the methyl radical and a hydrogen atom. On temperature increase from 373 to 600 K, the radical  $\text{CH}_3$  undergoes stepwise dehydrogenation



Schouten *et al.*<sup>56</sup> carried out experiments at 600 K and have proposed a similar scheme of the formation of surface nickel carbide:



Kinetic studies of methane decomposition were performed at 723–823 K in a catalytic reactor with a microbalance.<sup>57–59</sup> Analysis of the results obtained was based on the model of Grabke<sup>60,61</sup> according to which the decomposition of methane on  $\alpha$ -Fe and  $\gamma$ -Fe surfaces occurs as a result of successive splitting of hydrogen atoms, while the limiting step is the decomposition of the methyl radical. On the other hand, Alstrup and Tavares<sup>57,59</sup> showed that the limiting step could be both dissociative adsorption of methane and dehydrogenation of adsorbed methyl groups, whereas Snoeck *et al.*<sup>62</sup> state that this process is limited by the step of detachment of the first hydrogen atom from the methane molecule adsorbed on the nickel surface.

Our kinetic studies of methane decomposition on aluminium–nickel catalysts<sup>63</sup> showed that the activation energy of carbon formation on nickel decreases as the temperature increases. In the temperature range 798–873 K, the activation energy is  $75 \text{ kJ mol}^{-1}$ , which is close to the literature data [*cf.*

$88 \text{ kJ mol}^{-1}$  (Ref. 58),  $90 \text{ kJ mol}^{-1}$  (Ref. 59),  $96 \text{ kJ mol}^{-1}$  (Ref. 64) and  $97 \text{ kJ mol}^{-1}$  (Ref. 65)]. Apparently, the limiting step is dehydrogenation of the adsorbed methyl radical with formation of surface nickel carbide, which is confirmed by the study of the kinetics of nickel carbide formation from methane on the (110) face of a nickel single crystal.<sup>56</sup> The activation energy of the surface nickel carbide formation is  $87 \pm 12 \text{ kJ mol}^{-1}$  (see Ref. 56).

In the temperature range 923–1023 K, the activation energy of carbon formation from methane decreases to  $26 \text{ kJ mol}^{-1}$ . Similar values of the activation energy of carbon formation from methane ( $0$ – $40 \text{ kJ mol}^{-1}$ ) were obtained for the nickel-containing catalysts,<sup>66,67</sup> as well as for the (111) and (100) faces of nickel.<sup>50,51,68</sup> The value  $26 \text{ kJ mol}^{-1}$  coincides with the experimental  $E_a$ , which characterises the dissociative adsorption of methane on the face (100) of the nickel surface with formation of the methyl radical and a hydrogen atom.<sup>68</sup> This makes it possible to conclude that the limiting step of methane decomposition on nickel catalysts at 923–1023 K is the dissociative adsorption of methane with formation of a hydrogen atom and methyl radical.

## III. Regularities in the formation of carbon of different morphological types on iron subgroup metals

### 1. Varieties of carbon deposits

Carbon formed on the iron subgroup metals or their alloys with other metals is produced in the form of deposits possessing various crystallographic characteristics, which depend on the specific features of catalysts and conditions of the process. Using these dependences, one can purposefully control the technologies of preparation of carbon deposits of various morphologies.<sup>69</sup> Carbon can be deposited as filaments of different configuration, nanotubes, plates and other forms.

The most interesting varieties are characteristic of the forms of filaments. Figure 2 shows three basal structures of carbon filaments.

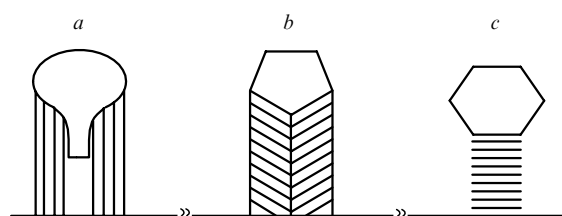


**Figure 2.** The structures of graphite filaments with different positions of basal planes;

(a) coaxial-cylindrical; (b) coaxial-conical; (c) flat-parallel (in the form of stacks of plates of graphite planes).

Carbon nanotubes have first been revealed as a concomitant product in the preparation of fullerenes by vaporisation of graphite in an electric arc.<sup>70</sup> It was shown later that nanotubes could also be obtained by catalytic methods.<sup>71–73</sup> Nanotubes differ from carbon filaments primarily in their smaller sizes. Carbon nanotubes consist of 1–50 cylindrical graphite-like layers coaxially inserted into each other;<sup>70,74,75</sup> the diameters of cylindrical cavities are 0.7–6 nm, whereas the lengths of the tubes reach several micrometers. In a chemical respect, the nanotubes obtained by graphite vaporisation differ from the known forms of carbon in their increased resistance to oxidation.<sup>76</sup>

### 2. Regularities of the formation of filamentous carbon

The growth of carbon filaments is catalysed by finely dispersed metal particles. The limits of sizes were established outside which the metal particles are coated with carbon and lose their abilities

to perform catalytic functions.<sup>77–80</sup> The lower limit is  $\sim 30 \text{ \AA}$ , while the upper limit depends on the coefficient of carbon diffusion in the bulk of the metal particle. For nickel and cobalt, these are  $\sim 1000\text{--}1500 \text{ \AA}$ . The carbon diffusion coefficient in iron is 2–3 orders of magnitude larger than that in nickel and cobalt; therefore, the upper limiting size of iron particles is at least one order of magnitude larger.<sup>79</sup>

The growth of carbon filaments on finely dispersed particles of the iron subgroup metals and their alloys with some other metals is a physical step of the carbide cycle mechanism.<sup>5, 6, 9–18, 77–79</sup> This process is to some extent unique and is of great interest for fundamental science.

The growth of carbon filaments was directly observed in the gas chamber of an electron microscope.<sup>33, 35</sup> The following regularities were revealed:

(1) a particle of a catalyst is present at the growing ends of each filament;

(2) the diameter of filaments is controlled by the size of the catalytic particle at the growing end, which is fragmented in most cases, and this initiates growth of finer filaments;

(3) the diameters of filaments range from 100 to 1500  $\text{ \AA}$ , while their lengths can reach  $8 \times 10^4 \text{ \AA}$ ;

(4) the grown filaments have various forms (loops, helices, interwoven mass);

(5) the dependence of the rate of filament growth on time is S-shaped;

(6) the time for the carbon filament formation depends on the reaction temperature: at 923 K, the growth of some filaments lasts for 10 min, while at 1243 K their growth stops after 30 s.

The catalytic particle at the end of the filament is pear-shaped.<sup>33, 35</sup> An electron-transparent channel often passes along the entire filament length to its top. Reasonably, the filament has an external layer which is more resistant to oxidation than the internal one. The thickness of the external layer makes up  $\sim 10\%$  of the outer diameter.

In order to understand the regularities of formation of carbon filaments, it is necessary to answer at least the following questions.

(1) Why carbon atoms are formed predominantly on one crystal face of a metal particle and crystallise into graphite structures on other faces?

(2) What are the driving forces for the migration of carbon atoms to the sites of graphite phase formation and what are the peculiarities of the mass-transfer of carbon atoms?

(3) What are the conditions for the appearance of the graphite phase crystallisation centres and specific features of these centres?

(4) How do the crystallographic and crystallochemical features of metal particles influence the properties of graphite structures formed on them?

(5) What possibilities exist for the targeted formation of graphitic phases of different morphological types?

There are two explanations of the reasons for the transfer of carbon atoms from the front part of catalytic particles where they are formed to the rear side where the filament grows. Some investigators presume that this transfer occurs owing to the diffusion of carbon atoms over the surface of the catalytic particle.<sup>81</sup> However, the more popular is another viewpoint according to which the growth of filamentous carbon occurs as a result of diffusion of carbon atoms in the bulk of the metal particle.<sup>33–35, 39, 82–91</sup>

The mechanism of filamentous carbon growth proposed by Baker *et al.*<sup>33, 35</sup> is presented schematically in Fig. 3. After formation of small metal particles on a support (Fig. 3 *a*), deposition of amorphous carbon takes place at the site of particle contact with the support (Fig. 3 *b*). The formation of amorphous carbon is explained by the gas-phase polymerisation of acetylene. At the same time, acetylene is decomposed on a metal particle surface, and the carbon atoms are dissolved in the bulk of the metal. Decomposition of acetylene and solubilisation of carbon are accompanied by heat release, and this creates temperature gradient along the particle. Owing to this gradient, carbon moves

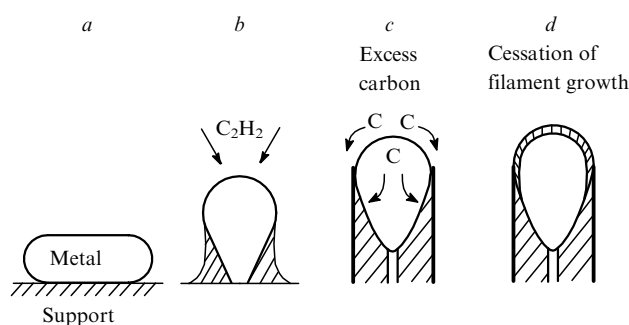


**Figure 3.** Schematic representation of the mechanism of the filamentous carbon growth from acetylene on a metal (see the text for comments).

to a colder part of the particle in contact with the support. The deposited carbon raises the metal particle and removes it from the support. The initial filament growth causes curvature of the metal particle which becomes pear-shaped, and this in turn leads to the formation of a channel (Fig. 3 *c*). The increase in the filament growth rate is explained by the insulation of the particle from the support and the corresponding increase in the temperature gradient. The excess carbon formed on the outer surface of the particle migrates from this surface and builds the external wall of the filament. It is presumed that the external wall of the filament has a different structure from that of its core. The filament growth stops when the 'hot' side of the particle is covered by carbon (Fig. 3 *d*).

In the authors' opinion,<sup>35</sup> their hypothesis is confirmed by the fact that the activation energies of the growth of carbon filaments on  $\alpha$ -Fe, Co, Cr and Ni are close to the activation energies of carbon diffusion in the bulk of the corresponding metal. However, the values of the growth rates of carbon filaments on different metals<sup>33, 35</sup> are contradictory. If the formation of filaments is governed only by the diffusion of carbon atoms in the corresponding metal, then under the same experimental conditions (1010 K, acetylene as the carbon source, catalytic particles of the same sizes), the growth rates should be proportional to the diffusion coefficient of carbon atoms in the corresponding metal. As noted above, the coefficient of carbon diffusion in metallic iron is 2–3 orders of magnitude larger than that in cobalt or nickel. Consequently, the rate of growth of carbon filaments on iron should be proportionally higher. However, in practice it proved to be lower on iron than on nickel or cobalt.<sup>33, 35</sup> In this context, it is reasonable to suggest that the limiting step on iron is the interaction of acetylene with the surface of the metal.

The driving force of diffusion was presumed<sup>33, 35</sup> to be the temperature gradient arising between the sites where the decomposition of hydrocarbons occurs and the sites where the graphite phase grows. The higher the metal temperature the larger the solubility of carbon in it; for this reason, concentration gradient also appears.

The concept according to which the growth of filamentous carbon is brought about by carbon diffusion in a crystal has been accepted by most investigators, whereas the appearance of mass gradient determined by the temperature gradient has become the subject of lively discussion.<sup>81, 82, 84–87, 92</sup> The arguments of the opponents were based on the fact that the hydrocarbons, the decomposition of which is an endothermic process (*e.g.*, methane), also provide the growth of carbon filaments. The suggestion according to which the deposition of carbon is explained by the presence of admixtures of other hydrocarbons in methane was disproved by the fact that with high-purity methane (99.99 vol.%) the degree of its decomposition reached 30%.<sup>87</sup>

In order to assess the magnitude of the temperature gradient, Tibbetts *et al.*<sup>93</sup> have simulated the process of the growth of the carbon filaments from acetylene on  $\gamma$ -Fe. To simplify calculations, they suggested that the filament has no hollow channel and its

diameter is equal to the diameter of the metal crystal initiating the filament growth. The thermal balance of the growing filament end was calculated on the assumption that all the heat released in the decomposition of hydrocarbons is absorbed by the metal particle. Calculations showed that the temperature gradient is smaller than  $2 \times 10^{-3}$  K, and such a small magnitude cannot ensure the really observed growth rates of carbon filaments. Nonetheless, unsuccessful attempts were undertaken to prove a substantial influence of the temperature gradient.<sup>94–96</sup>

An alternative explanation of the nature of the driving force of diffusion is based on the appearance of concentration gradient. In the model proposed by Rostrup-Nielsen and Trimm,<sup>97</sup> it was suggested that the solubility of carbon at the hydrocarbon–metal boundary is higher than that at the metal–graphite boundary. However, the data on solubility used in this model and based on the results reported by Wada *et al.*<sup>88</sup> are questionable.

The hypothesis of concentration gradient was also supported by the authors of a series of studies,<sup>98–100</sup> who investigated the growth of filamentous carbon upon disproportionation of CO on Co/Fe alloys. It was presumed that the activity of carbon at the gas–metal interface is determined by the carbon activity in the gas phase. The activity of carbon at the metal–filament interface was assumed to be equal to the activity of graphite. On the basis of this simple assumption, a kinetic equation was deduced according to which the rate of carbon deposition depends linearly on the carbon activity in the gas phase. However, the explanation of the reasons for the appearance of the concentration gradient<sup>97–100</sup> appears to be supported with insufficient argumentation.

Based on the carbide cycle mechanism, a model of the filamentous carbon growth was constructed which does not contradict most experimental results.<sup>5,6,15</sup> We believe that the mass-transfer of carbon atoms occurs owing to their diffusion in the bulk of metal particles from the formation site to the crystallisation centres. Depending on the ratios of the rates of formation and diffusion of carbon atoms, the limiting steps of the process may be different. Let us consider the growth of carbon filaments under the conditions where the limiting step is the diffusion of carbon atoms in the metal particle.

In a saturated solution, the solid and dissolved phases possessing equal chemical potentials are in equilibrium. In our case, however, carbon on the front and rear sides of the metal particle is in different states which are characterised by different chemical potentials. The pool of carbon on the front side of the particle is continually replenished due to the decomposition of hydrocarbons. On the rear side, carbon is formed as the graphite phase. The concentrations of saturation (solubility) of carbon at these sites are substantially different; therefore, a concentration gradient arises, which ensures continuous dissolution of carbon on the front side and its diffusive mass-transfer to the rear side of the metal particle. This gradient is rather high. The concentration of carbon atoms on the front side of the nickel particle formed by decomposition of intermediate carbide-like compounds is close to the concentration of carbon in Ni<sub>3</sub>C carbide, *i.e.*, it reaches 25 at. %. This value is confirmed by the calculation of the linear rate of carbon filament growth.<sup>15</sup>

The linear rate of the carbon filament growth ( $V$ ) is determined by the amount of carbon  $Q$  which has diffused through an area section unit of a metal particle in unit time.

$$Q = \frac{D(c_1 - c_2)}{L} \quad \text{and} \quad V = \frac{D(c_1 - c_2)}{Ld},$$

where  $D$  is the coefficient of carbon diffusion in the metal,  $c_1$  is the carbon concentration in the surface carbide-like compound,  $c_2$  is the carbon concentration in the saturated solution of carbon in nickel on the rear side of the metal particle,  $L$  is the diameter of the metal particle at the end of the filament,  $d$  is the density of graphite.

These formulae were used to calculate the rates of the growth of carbon filaments 600 Å in diameter on metallic nickel at 873 K.

Decomposition of an intermediate carbide-like compound of the Ni<sub>3</sub>C type gives the concentration  $c_1 = 0.514 \text{ g cm}^{-3}$ ; the values of  $c_2 = 3.8 \times 10 \text{ g cm}^{-3}$ ,  $D = 3.89 \times 10^{-10} \text{ cm}^2 \text{ s}^{-1}$ ,  $d = 2 \text{ g cm}^{-3}$  were taken from the monograph of Buyanov.<sup>5</sup> The growth rate of carbon filaments found ( $1650 \text{ Å s}^{-1}$ ) is close to the values measured experimentally<sup>33,34</sup> ( $800–1600 \text{ Å s}^{-1}$ ).

An analogous explanation of the reasons for the diffusion of carbon atoms in the metal particle is given in Refs 101–107.

At present, the concept of the formation of carbon filaments by carbide cycle mechanisms is commonly accepted for the iron subgroup metals and their alloys.<sup>108</sup>

### 3. The effect of the orientation of faces of metal single crystals on the growth of carbon filaments

Detailed crystallographic studies of the role of the orientation of catalytic particles in the preparation of filamentous carbon were carried out by Audier *et al.*<sup>98–100,109–115</sup> using mainly the disproportionation reaction of CO on Fe–Co and Fe–Ni alloys. It turned out that on all alloys with the body-centred cubic (BCC) structure, the carbon filaments are formed; the metal particles which initiate their growth are oriented in such a manner that the direction [100] of single crystals is parallel to the filament axis. The (100) face of the crystal is free from carbon. The alloys with the face-centred cubic (FCC) structure also catalysed the growth of filaments; however, they had a different orientation relative to the carbon filament. The direction [110] of crystals was always parallel to the filament axis.

Electron microscopy studies of the metal particle–filamentous carbon interface showed<sup>98–100,109–116</sup> that the liberation of carbon and generation of graphite layers occur on the vicinal faces of the catalyst particle. Near the metal–carbon interface, the graphite planes are arranged essentially parallel to the metal surface. The experiments were performed under the following conditions: the gas phase was compressed (75% CO and 25% CO<sub>2</sub>), the pressure was  $10^5$  Pa and the temperature range was 723–923 K.

However, an investigation of the structure and texture of the filamentous carbon obtained from benzene on iron and from buta-1,3-diene on nickel showed<sup>77</sup> that the particles of metallic iron are oriented differently relative to the filament axis. The iron particles which initiated the growth of filaments were single crystals in which it was the direction [110] that was parallel to the filament axis. Analogous results were obtained later by Rodríguez *et al.*<sup>117</sup> In crystals of metallic nickel the direction [100] was parallel to the filament axis, while the planes (100) and (110) were free from carbon. Similar orientation and disposition of faces were established by Yang and Chen.<sup>94</sup> Such an orientation of metal crystals and the presence of low-index faces in them are not occasional. Different faces possess different activities in the decomposition of hydrocarbons; the diffusion rate of carbon atoms through single crystals of metals can also be anisotropic.<sup>77</sup>

Thus, different faces and sites of the surface of metal crystals where the mechanism of the carbide cycle of decomposition of hydrocarbons is valid are not equivalent and they exhibit different properties in the general process of formation of carbon deposits. The distinction between the adsorption and catalytic properties of different faces and surface sites is confirmed by numerous data. For example, in the studies of methane decomposition on nickel in the temperature range 300–773 K it was found<sup>56,118,119</sup> that this reaction proceeded only on the faces (100) and (110) [but not on the (111) face]. At temperatures up to 673 K, surface carbide structures are formed on the surface of these faces and diffusion of the carbon formed in the bulk of nickel crystal becomes noticeable above 573 K. No chemisorption of methane or formation of carbon on the (111) face could be detected.

Decomposition of ethylene on the nickel faces (111), (110) and  $5(111) \times (110)$  is yet another example.<sup>120</sup> On the stepped faces  $5(111) \times (110)$ , the cleavage of bonds occurs in the lower temperature range than on the smooth faces (111) and (110).

Presumably,<sup>77–79</sup> the generation of the graphite phase is easier on the face (111) than on the faces (100) and (110) because of high degree of its geometric correspondence to the structure of the basal graphite plane. This conclusion is in good agreement with the results reported by Eizenberg and Blakely<sup>121</sup> who studied the isolation of carbon from a supersaturated Ni–C solution on the faces (111), (311), (110), (210) and (110) and the vicinal high-index surfaces of nickel. In the course of the monolayer filling, the vicinal surfaces of nickel are spontaneously restructured (faceted) into stepped faces formed by the terraces (111) and the monoatomic steps (110) or (310) depending on the index of the initial face.

#### 4. Steps of the growth of carbon filaments from methane on nickel-containing catalysts

Four individual sites (stages) which differ in the features of the carbon filament growth can be distinguished on the kinetic curves describing the decomposition of methane on the catalyst containing 85 mass % of Ni/Al<sub>2</sub>O<sub>3</sub><sup>122</sup> at 823 K. Analogous stages were observed in the formation of carbon from acetylene.<sup>27</sup>

Crystals of nickel of various shapes are formed after the reduction of an aluminium–nickel catalyst. In conformity with the carbide cycle mechanism, the carbon atoms liberated as a result of methane decomposition in the induction period of filament growth diffuse into the bulk of the metal and form there a supersaturated solution of carbon in nickel relative to the graphite phase. As soon as the critical level of supersaturation is reached and a crystalline graphite nucleus appears at some site, condensation of the carbon atoms from the supersaturated solution occurs on the nucleus formed. In this case, the concentration of dissolved carbon in the zone adjoining the graphite phase decreases to its level in the saturated solution. The (111) faces of nickel are the most favourable for the formation of graphite nuclei, since the symmetry and parameters of the flat networks (111) of nickel (Fig. 4a) and (002) of graphite coincide. The graphite filaments formed upon carbonisation of Ni/MgO or Ni/Al<sub>2</sub>O<sub>3</sub> catalysts have a coaxial conical structure where the graphite (002) layers are inserted one into another as funnels (see Fig. 2b). The correspondence of the structures of the face surface of nickel particles and the graphite filament can serve as a virtually classical example. It was shown<sup>63</sup> that the frontal side of a nickel crystal is formed by the (100) and (110) faces, while the faces (111) form its rear part.

After the appearance of the graphite crystallisation centres, the growth of graphite filaments begins, which is accompanied by the reconstruction of metal particles. During this period, the rate of carbon formation comes to stationary level. The shape of the metal crystals depends substantially on the rate of liberation of carbon atoms, their mass-transfer and specific features of the graphite structure.<sup>122</sup> The more intense the process the more labile is the structure of the metal particle.

Boellaard *et al.*<sup>105</sup> noted that the formation of carbon filaments with the coaxial-conical structure should result in slippage of the carbon layers relative each other. Due to irregular supply of carbon atoms to the back, rear side of a cone-like metal particle, the carbon layers lose the form of ideal cones, and the body of filaments acquires an imperfect graphite structure with numerous

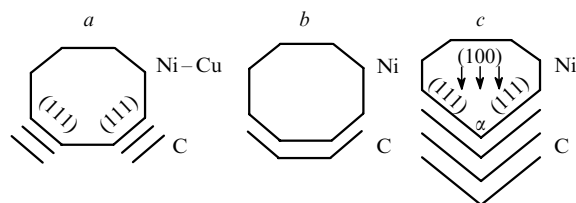


**Figure 4.** Schematic representation of a mechanism of the generation and growth of carbon filaments on Ni–Cu and Ni catalysts (see the text for comments).

defects, in particular with a considerable number of edge dislocations.

However, in our opinion, as the new graphite layers grow, the nickel particle should be lifted a little, while the (111) face of nickel and the basal graphite face should slide relative each other. Each new graphite plane slides to the central part of the carbon filament. Owing to high mobility of nickel atoms at the Ni–C interface, the surface metal atoms dislocate towards the filament axis, and this explains considerable transformation of the metal particle during the accelerated growth of the carbon layer observed on kinetic curves. In this case, the nickel particle (Fig. 4b) changes its shape (Fig. 4c). According to the crystallographic laws, the angle  $\alpha$  between the faces (111) should be approximately equal to 71°. However, at 823 K the transfer of nickel atoms out to the ‘tail’ of the crystal occurs rather strongly, which decreases the angle  $\alpha$  to 50–60°. It may be suggested that the relief of the above-mentioned faces is determined by the atomic steps which change the slope of the plane. The nickel particles which initiate the growth of filamentous carbon from methane on Ni/Al<sub>2</sub>O<sub>3</sub>, are well formed (see Fig. 4c). The face (100) is oriented towards the filament growth, while the faces (111) in the ‘tail’ part of the nickel crystal form a pyramid with its top facing the side opposite to the filament growth direction.<sup>63</sup>

It is clear that after the induction period the appearance of new crystallisation centres at some sites of the metal surface becomes virtually impossible. As a result, the site where the graphite growth occurs becomes the back (rear) side of the particle, while all the other faces, which are not closed by graphite, begin to play the role of the front side on which methane is decomposed by the carbide cycle mechanism. At relatively low temperatures of 748–798 K, such a form of nickel crystal remains invariable for a long time, which ensures stable growth of filamentous carbon. This stage is associated with the steady-state period of the filamentous carbon growth.

The velocity of filamentous carbon growth from methane at 823 K was estimated on the basis of the rate of carbon formation. Rather simple calculations<sup>122</sup> showed that the mean filament growth velocity is 6 Å s<sup>-1</sup>, while the carbon concentration on the front side of the nickel particle is only 2–3 times higher than that in the saturated solution in nickel at 823 K. It should be remembered that these results refer to the decomposition of the most stable hydrocarbon, *viz.*, methane. Therefore, in this case the limiting step is the decomposition of CH<sub>4</sub> molecules rather than the diffusive transfer of carbon atoms in the bulk of nickel particles. If the growth of filaments is limited by the diffusion of carbon in the bulk of the metal, then, as it was shown above, the gradient of carbon concentration becomes extremely large. This gradient predetermines the magnitude of diffusive flux of carbon atoms in the metal particle and has a strong effect on the phase state of the metal.

Transition metals (Fe, Co, Ni) have small atomic radii. In particular, it is 1.24 Å for nickel, and for this reason, the carbon atom with a radius of 0.77 Å is too large to occupy the octahedral voids of the most dense FCC-packing of nickel. Thus, diffusion of carbon through the nickel particle results in distortion of the crystal lattice of the latter. In some cases, the catalytic particle can become highly labile owing to a high carbon concentration, intense motion of carbon atoms through the metal bulk and the release of heat upon their condensation in the form of graphite phase.

Centres of carbon crystallisation on the metal particle are formed if a high energy barrier, which is 170 kJ mol<sup>-1</sup> for nickel<sup>123</sup> and 220–300 kJ mol<sup>-1</sup> for iron, is overcome.<sup>17</sup> This is possible owing to a considerable supersaturation of carbon solutions in the metal which is especially large in the early stages of hydrocarbon decomposition. Studies using a high-temperature X-ray chamber showed<sup>124</sup> that in the course of induction period the concentration of carbon atoms on nickel exceeds 2 at.%.

Based on a thermodynamic analysis, Parmon<sup>125</sup> concluded that owing to a strong supersaturation of iron or nickel with

carbon, which can reach  $> 10$  mass %, melting of the metal should begin at  $\sim 920$  K. In our opinion, this relates primarily to the induction period of the filamentous carbon growth because after the formation of graphite nuclei the maintenance of such a high carbon concentration in the metal is hardly probable.

The formation of carbon filaments is often associated with the high mobility of metal-carbon particles. In this connection, one should mention the VLS (vapour-liquid-solid) mechanism proposed for the description of the growth of silicon filaments on drops of a liquid metal.<sup>126</sup>

The problem of the possibility of melting of metal particles has not been totally solved yet, and the temperature boundary where the metal particles catalysing the growth of filamentous carbon or nanotubes can pass to the liquid state, has not been established yet. Some authors state<sup>127, 128</sup> that the finely dispersed catalytic particles of iron are capable of melting even at temperatures below 1173 K. They believe that the particles of liquid iron are 'responsible' for the efficient growth of carbon filaments. However, according to other data (see, *e.g.*, Refs 129 and 130), the 'liquefaction' of iron particles occurs at  $\sim 1400$  K.

Relevant calculations confirm that the growth of carbon filaments from methane is initiated by edged particles oriented in a definite manner relative to the filament axis; the growth of carbon filaments from alkenes, dienes and acetylene is initiated by the pear-shaped particles, the form of which is less expressed.

In the so-called 'extrusion' method, which is less common than the above-considered (classical) method for the formation of carbon filaments, the crystal initiating the carbon deposition remains in contact with the support. This process occurs in the growth of carbon filaments on Pt/Fe alloys<sup>36</sup> and on pure metals.<sup>35, 131, 132</sup>

### 5. Specific features of the formation of carbon filaments on metallic iron

In a number of cases, deposits of carbon on iron catalysts have the form of filaments.<sup>77</sup> A general view of such filaments is shown in Fig. 2*a*. Figure 5 shows a micrograph of one such filament. As a rule, the carbon filament contains inclusions both at end of the filament and in its hollow channel, which, according to micro-



**Figure 5.** A micrograph obtained by the method of high-resolution electron microscopy (HREM) of a carbon filament formed on metallic iron from an atmosphere of benzene diluted with argon in the molar ratio  $C_6H_6 : Ar = 1 : 15$  at 923 K.<sup>77</sup>

diffraction data, represent the metal phase. Reflexes on electronograms indicate that this phase has a body-centred cubic lattice of  $\alpha$ -Fe. The characteristic feature is that the crystallites which are constituents of the filament structure are oriented in a definite manner relative to its axis. The crystallographic direction of  $\alpha$ -Fe [110] is parallel to the axis. The metallic inclusion at the end of the filament has usually the drop-like form, which is narrowed in its lower part and is weakly edged. The inclusions have a block structure. This follows from the existence of boundaries between the blocks as seen on electron micrographs and from the periodic contrasting of the areas of overlap of individual blocks.

The carbon of the filament is graphitised, and this is clearly seen in micrographs obtained by the high-resolution electron microscopy method. The distance between the planes is  $3.5 \pm 0.2$  Å, which is close to the interplanar distance  $d_{002}$  for graphite. Zaikovskii *et al.*<sup>77</sup> showed that the graphite layers are concentrically arranged around the filament axis and the inter-channel metal particle.

The distribution of carbon around the metal particle at the end of the filament is irregular. The smallest thickness of the carbon layer (only a few monolayers) is observed on the side of the metal particle where the decomposition of a hydrocarbon occurs. As the distance from the top of the metal particle increases, the thickness of the carbon layer increases. The orientation of graphite layers at different sites of the metal surface is also different. In contrast to the upper part of the metal particle, in its lower part the graphite layers form a certain angle with the surface and are in contact with the metal by their terminal sides (Fig. 2*a*).

In the hollow channel of the filament there are very thin (2–10 monolayers) partitions composed of carbon layers.

Note in conclusion that the mechanism of generation and growth of carbon filaments on  $\alpha$ -Fe is extremely complex. When considering these processes, one should take into account the following characteristic features of carbonisation of metallic iron:

- (1) high diffusion coefficient of carbon in the bulk of the metal ensuring its rapid supply to different surface sites;
- (2) incomplete epitaxial correspondence between the parameters of  $\alpha$ -Fe face (111) and the basal graphite plane (002), which impedes the formation of nuclei of the graphite phase.
- (3) the tendency of metallic iron to form carbides.

### 6. Regularities of the formation of carbon deposits in the 'octopus' form

On nickel-copper alloys, the formation of unusual morphological 'octopus' carbon was observed.<sup>63, 106, 133–135</sup> One particle of nickel-copper alloy initiates the growth of several filaments in different directions (Fig. 4*a*).

In contrast to nickel, metallic copper has low activity in the processes of carbon formation. It was used as an additive to Ni/MgO and Ni/Al<sub>2</sub>O<sub>3</sub>, because it has the same face-centred lattice like nickel and forms alloys with nickel in a wide range of concentrations. After reduction by hydrogen of the catalyst containing 10 mass % of MgO, 12 mass % of Cu and 78 mass % of Ni, the X-ray patterns reveal the predominance of the lines of MgO and a nickel-copper alloy of cubic structure<sup>63</sup> with the unit cell parameter  $a = 3.53$  Å; this parameter corresponds to an alloy of approximate composition Ni<sub>0.9</sub>Cu<sub>0.1</sub>. The mean size of the alloy particles found from the half-width of the line (311) is 210 Å.

Kinetic studies of the formation of carbon from methane on the catalysts Ni/MgO and Ni-Cu/MgO showed that the rate of this process decreases as the content of copper in the sample increases.<sup>63</sup> Addition of 12 mass % of copper decreases this rate 2–3-fold. As a result, the aggregation of carbon atoms proceeds in a more ordered manner, and one observes a rather clear-cut trend towards the formation of graphite on the (111) face of the nickel-copper alloy (see Fig. 4*a*). The lattice parameter of the alloy increases with the increase in the copper content, and the crystallographic correspondence of the (111) faces of the alloy and the faces (002) of graphite becomes more and more complete.

Electron microscopy analysis showed<sup>63, 79, 133</sup> that carbonisation of the Ni–Cu/MgO catalyst upon decomposition of methane for 1 min at 873 K leads to the formation of carbon filaments, the ends of which contain metal particles. This metal particle usually has a well edged form, while its diameter exceeds the diameter of the carbon filament. The data from electronic microdiffraction (EMD) suggest that the (111) face of the FCC lattice of the metal is the most developed. It is perpendicular to the direction of the filament growth and is in contact with the (002) planes of graphite. The lateral (100) faces of the alloy are free, they have no contact with carbon and are the centres of methane decomposition. The form presented in Fig. 4a corresponds to the initial stage of the growth of filamentous carbon on particles of the Ni–Cu alloy.

Carbon can be formed simultaneously on two opposite faces (111) of the flattened alloy particle; this can give birth to two carbon filaments in the form of rings containing a metal particle inside. Sometimes, carbon is deposited simultaneously on three (111) faces of a nickel–copper alloy and the growth of filaments begins in three directions (Fig. 6). According to the data from EMD, the structure of such filaments is formed by the graphite layer (002), arranged perpendicularly to the filament growth direction.<sup>63, 79, 133</sup>

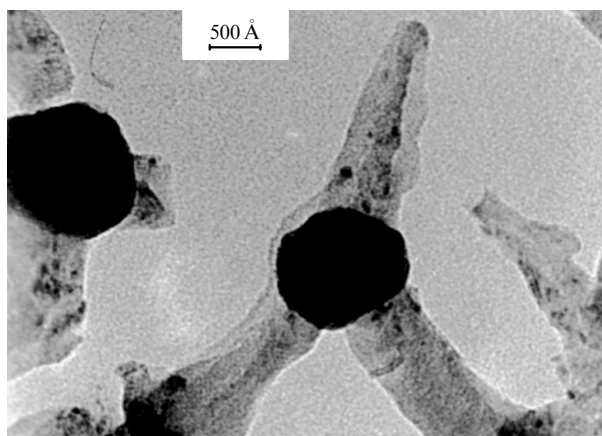


**Figure 6.** A micrograph showing the filamentous carbon growth in three directions on the Ni–Cu alloy particles.<sup>63</sup>

The sizes and shapes of faces which determine the equilibrium habits are known to be related to the surface energies of these faces. The difference in the habits of catalytically active particles in nickel and nickel–copper catalysts is explained by different degrees of proximity of the parameters of hexagonal lattices of the nickel and nickel–copper alloys to the parameter of the graphite lattice. The link of carbon with a particle of nickel–copper alloy over the face (111) is stronger; consequently, the surface energy in this case is lower than on the nickel particle, and the size of (111) face is increased.

After carbonisation with methane for 2 min at 873 K the particles lose their clearly expressed edging.<sup>63</sup>

The increase in the carbonisation time to 5 min induces changes in the structure of metal particles. It becomes of micro-block-type, the size of the blocks being 50–200 Å. The defectiveness of the alloy surface deteriorates the ordering of the graphite layers formed and in some places the filament is separated into layers (Fig. 7). This favours the formation of bundles of filaments growing from one particle. Very often, thin branches appear from the major bundle or from the block-polycrystalline metal particle. At the ends of such branchings, there are also metal particles.<sup>63, 79</sup>

Carbon deposits, formed on the Ni–Cu/MgO catalyst upon decomposition of CH<sub>4</sub> for 3 h at 875 K present a porous mass consisting of filaments intertwined in a complex manner. In

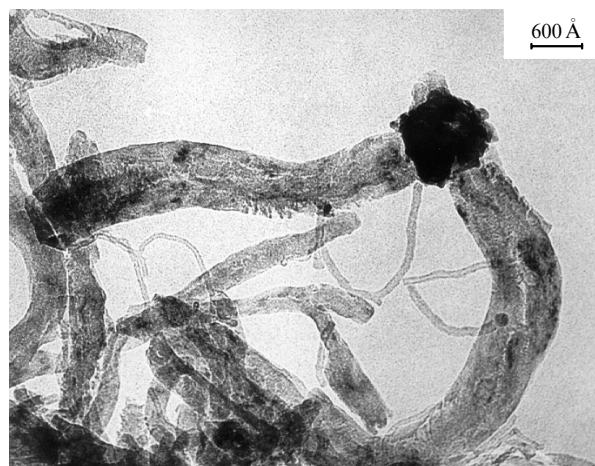


**Figure 7.** Morphology of the carbon formed from methane on the block particle of Ni–Cu alloy after a 5-min relaxation at 873 K.

addition to large filamentous formations, numerous thin filaments 50–100 Å in diameter are present. Taking this into account, it may be concluded that large particles of the alloy break into individual blocks which catalyse the growth of thin filaments.

Thus, one of the stages in the formation of carbon deposits is the diffusion of carbon atoms in the metal particle determined by different concentrations of these atoms near those faces where a hydrocarbon is decomposed and graphite is condensed. The directed diffusion of carbon atoms at elevated temperatures leads to the displacement of the matrix atoms (Cu and Ni). This effect is the stronger the higher the ability of components to form chemical bonds with carbon. Stratification and fragmentation of a single crystal of the initial alloy in the process of the carbon filament growth may be explained by bulk diffusion of atoms. Consequently, as the carbon accumulates, the morphological structure of the carbon mass begins to resemble a branched tree.<sup>63</sup>

### 7. The reasons for deactivation of a catalytic particle in the growth of a carbon filament

The phenomenon of deactivation of catalysts in their carbonisation by hydrocarbons has been investigated.<sup>5, 136</sup> Deactivation is caused by destruction and grinding of catalysts, removal of some components from them and by the mechanical capture of individual microparticles by the growing carbon filaments. This phenomenon was called carbon erosion.

Electron microscopy studies of carbon filaments which ceased to grow showed that the front side of nickel particles is covered by a carbon film. Treatment of such filaments with hydrogen or oxygen leads to the recovery of their activity and continuation of growth.<sup>27</sup>

In our view, the cessation of the filamentous carbon growth is explained by the peculiarities of the process itself. As noted above, the diffusion of carbon atoms in the nickel particle is determined by the existence of a concentration gradient. The concentration of carbon on the faces (100) and (110) on the frontal side of the crystal is larger than its equilibrium concentration at the nickel–graphite interface. Supersaturation of carbon solution in the metal is the driving force of structural transformations on the surface of nickel. The larger the supersaturation the faster the deactivation.

Wesner *et al.*<sup>137</sup> considered surface autodiffusion of carbon atoms on the (100) face of a nickel single crystal which is induced by catalytic hydrogenation of CO with the formation of methane. On this face, sinusoidal grooves 1 μm deep were made at a distance of 7 μm. After the catalytic hydrogenation of CO for 6 h, the shape of the section profile changed substantially. Faceting of the groove was spreading from the ridge down to the

'valleys'. Taking this into account, it may be suggested that the nickel atoms dislocate from the 'valleys' in the direction of ridge peaks with simultaneous creation of cutting. The height of ridges increases with time. There are grounds to believe that in the process of carbon deposition reconstruction occurs of the surface of the front side of the metal particle, on which the steps corresponding to the (111) faces appear. Thus, conditions are created for the formation of new graphite nuclei on the front side of the nickel crystal. Therefore, the front side of the nickel crystal becomes coated with a thin carbon film with time despite the efflux of carbon atoms inside the crystal. This is the primary mechanism of deactivation of metal particles which catalyse the growth of carbon filaments.

One manifestation of the carbon erosion is the destruction of metal particles initiating the growth of carbon filaments with the formation of smaller and smaller fragments which can eventually be totally 'overgrown' with carbon and become isolated. A spectacular example may be the above-described growth of filamentous carbon on the Ni–Cu alloy particles in the Ni–Cu/MgO catalyst. The initially formed filaments 500–1000 Å in diameter are branched with time. This is due to the fact that the diffusion flux of carbon atoms in the bulk of alloy particles favours their fragmentation and crushing into subcrystals, a part of nickel being removed with carbon. As the initial particle is fragmented, a deposition of carbon begins not only on major filaments, but also on the surfaces of a contact between individual subcrystals. As a consequence, the initial particles undergo the ever-increasing splitting, while each new smaller particle becomes the centre of the growth of new filaments of a smaller diameter. Gradual extinction of the process of carbon deposition is explained by the fact that the metal particles of some minimal size prove to be covered by a graphite envelope and are switched off the process.

### 8. The effect of carbonisation temperature on the regularities of growth of carbon filaments in the decomposition of methane on nickel and nickel–copper catalysts

The increase in the reaction temperature influences the peculiarities of the filamentous carbon growth on both nickel and nickel–copper catalysts. Figure 8 shows the kinetic curves of carbon formation from methane at different temperatures on an Ni–Cu/MgO catalyst (analogous kinetic curves were also obtained for an Ni/MgO catalyst).<sup>122</sup> The rate of carbon formation increases with temperature. However, at 973 K the higher rate is maintained only for a few minutes, after which it drops abruptly. Figure 9 shows an electron micrograph of a filamentous carbon obtained from methane at 1023 K on an Ni/Al<sub>2</sub>O<sub>3</sub> catalyst. It is seen that the nickel particles appear to stretch along the filament length. As a result, the channel inside the carbon filament is filled with metallic nickel. Analogous morphology is also characteristic of the filamentous carbon obtained from

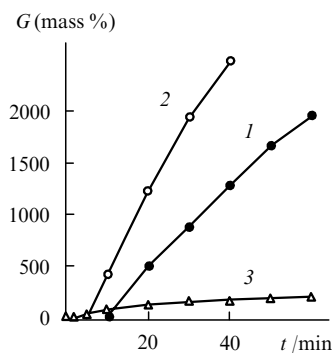


**Figure 8.** Kinetic curves of the carbon formation from methane on an Ni–Cu/MgO catalyst at 823 (1), 873 (2) and 973 K, respectively. *G* is the carbon increment.



**Figure 9.** A micrograph of the filamentous carbon formed from methane on an Ni/Al<sub>2</sub>O<sub>3</sub> catalyst at 1023 K.

methane on an Ni–Cu/MgO catalyst at 973 K. A question arises: what is the reason for the internal cavity formation in the graphite filament and what forces 'drag' the metal particle along this cavity?

The second mechanism of deactivation of metal particles which catalyse the growth of carbon filaments consists in the following. The increase in temperature and the higher rate of the filamentous carbon growth lead to an increase in the viscous fluidity of the metal particle, which facilitates sliding of the graphite planes formed over the surface of the metal<sup>122</sup> and intensifies the efflux of nickel atoms in the direction of the diffusion flow of carbon atoms, *i.e.*, into the 'tail' part of the metal particle. As a result, the particle is elongated, while the angle  $\alpha$  (Fig. 10 *a*) decreases considerably; the catalytic particle is transformed (Fig. 10 *b*). In the limit, the particle is so elongated that it acquires the shape of a needle (Fig. 11). Since in this case, the (111) faces become virtually parallel, the graphite deposited on them does not push the nickel crystal ahead but rather brings about lateral compression, which makes it still more elongated. Because of a large length of the nickel needle, the accumulation of carbon and supersaturation of the tail part in it proceed slowly. After reaching the critical supersaturation of the tail part of the nickel crystal, rapid condensation of carbon atoms begins with the formation of graphite layers which create carbon partitions inside the filaments. This in turn leads to irregular forward movement of the metal needle by pulsation. This results in the periodic appearance of carbon partitions which are seen in Fig. 11.

However, the situation changes considerably if carbonisation is carried out at 973 K in an atmosphere of methane diluted with hydrogen in the molar ratio 1:1. The morphology of the filamentous carbon formed on both Ni/Al<sub>2</sub>O<sub>3</sub> and Ni–Cu/MgO

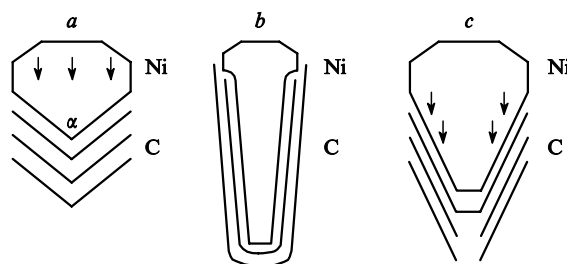


**Figure 10.** Transformation of catalytic particles upon the reaction temperature increase (see the text for comments).

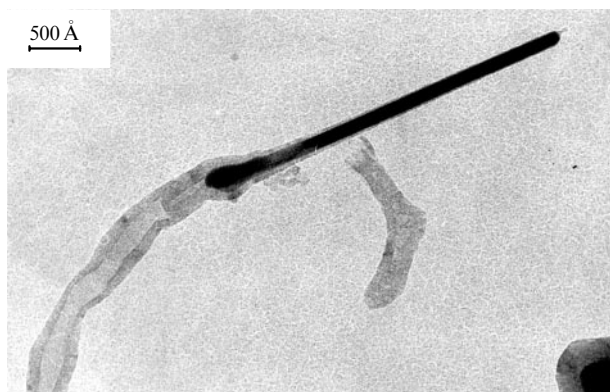


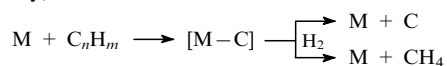
**Figure 11.** A micrograph of the filamentous carbon formed from methane on the Ni–Cu/MgO catalyst at 973 K.

becomes different. A hollow channel appears inside the carbon filament. (Fig. 10 *c*).

We have already mentioned that as the intensity of the process increases, the probability of restructuring of the metal becomes higher until some faces disappear and the other faces develop. In this case, upon addition of hydrogen to methane, the methanation of carbon atoms on the front side becomes possible. In other words, the reaction takes place which is opposite to methane decomposition, the carbon concentration on the front side decreases and the entire process is slowed down. It is logical to suggest that in this labile system reconstruction of the structure shown in Fig. 10 *a* into the structure shown in Fig. 10 *b* occurs. On the rear, a less active face (100) is formed in the side outgrowth; this is surrounded by more active sites (111).<sup>111, 113</sup> The carbon is predominantly deposited at the sites marked with the arrows in Fig. 10 *c*, and this determines the speed of the motion of the entire particle. Thus, the reason for the appearance, along the filament axis, of a hollow channel the diameter of which is commensurable with the size of the 'passive' face (100) on the rear side of the particle is the stretching of the catalytic particle. Baker and Harris<sup>27</sup> explained the formation of a hollow channel by the slower supply of carbon atoms because of the increase in its diffusion route. However, this is rather the consequence of the catalytic particle stretching. The graphite layers which arise slowly on this face are sealed off periodically, making partitions in the hollow of the channel. At a more rapid influx of carbon atoms, the hollow channel should have filled with carbon.

### 9. The effect of hydrogen on the formation of carbon filaments

The knowledge of general regularities and specific features of the carbide cycle mechanism allows prediction of the influence of hydrogen on the deposition of carbon. Hydrogen can hydrogenate metal (M) carbides with the formation of lower hydrocarbons, mainly, methane:



Owing to this property, hydrogen also affects the formation of carbon; in the case of nickel, this effect is stronger than in the case of cobalt or iron.

Upon dilution of buta-1,3-diene with argon alone, the carbonisation of nickel proceeds rapidly at the beginning of the reaction, but then the rate of carbon deposition drops abruptly (Fig. 12). Addition of hydrogen decreases the initial rate of carbon formation. The larger the partial pressure of hydrogen in the reaction mixture the stronger is this decrease. At a partial hydrogen pressure  $p_{H_2}$  of 17.5 kPa, the rate becomes constant and does not depend on the carbon content on the catalyst. At higher pressures, an induction period appears the duration of which increases with

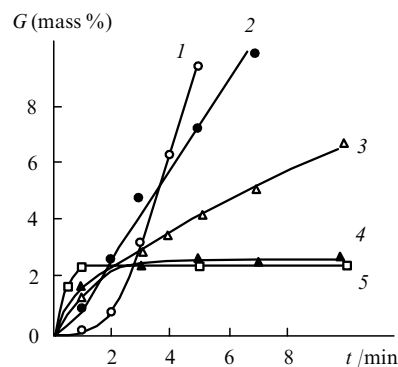


**Figure 12.** Effect of hydrogen on carbonisation of nickel by buta-1,3-diene at 698 K. The partial pressure of hydrogen/kPa: (1) 26.2; (2) 17.5; (3) 8.8; (4) 3.5; (5) 0.

$p_{H_2}$ . If a hydrocarbon is diluted with hydrogen 300 times, the induction period will become so long that carbon will not be formed over 2 h.<sup>138</sup>

An electron microscopy study showed<sup>123</sup> that carbon deposits formed upon dilution of a hydrocarbon with argon or hydrogen to  $p_{H_2} = 17.5$  kPa, present mostly a film which screens the nickel surface. At a higher hydrogen pressure, carbon is deposited in the form of filaments which do not block the surface.

When carbonisation occurs in the medium of a pure or argon-diluted hydrocarbon, favourable conditions are provided for the appearance of the graphite nuclei, since in this case the carbon atoms do not have enough time to escape from the place of hydrocarbon decomposition. During subsequent growth of the nuclei, these atoms form a regular layer blocking the nickel surface.

Upon partial or complete replacement of an inert diluent by hydrogen, hydrogenation of an intermediate carbide-like compound begins to occur in addition to the hydrocarbon decomposition. At the same time, hydrogenation of carbon with atomic hydrogen formed as a result of the dissociation of  $H_2$  molecules on the nickel surface becomes possible. As the partial pressure of hydrogen is increased, the hydrogenation rate increases. This decelerates the formation of the carbon phase nuclei on the surface accessible to hydrogen and leads to the appearance of an induction period. The activation energy of the graphite nuclei formation is  $170 \text{ kJ mol}^{-1}$  during the deposition of the first 1%–2% of carbon on nickel.

In a hydrocarbon–hydrogen medium, such nuclei are formed on the surface to which the access of reagents is hampered since hydrogen hydrogenates both the carbon atoms formed and the graphite nuclei. Owing to diffusion, a portion of carbon atoms is transferred to the interblock boundaries of nickel microcrystallites where new graphite nuclei are formed on defects.

Deposition of carbon on the interblock boundaries of nickel crystallites favours their dispersion and increases the number of metal particles which are actively involved in the interaction with the reaction medium. After the induction period and with the accumulation of graphite nuclei, the activation energy of carbon formation decreases and becomes constant ( $140 \text{ kJ mol}^{-1}$ ) after deposition of 10% of carbon. The transfer of carbon to the graphite phase nuclei (diffusion of carbon atoms in the metal bulk) becomes the limiting step of carbonisation. The value  $140 \text{ kJ mol}^{-1}$  is close to the reference value of the activation energy of the diffusion of carbon atoms in nickel.

Fragmentation of polycrystalline nickel into particles coated with carbon on the side inaccessible to the gas medium creates prerequisites for the formation of filamentous carbon. In this case, the carbon constituting the growing filament is not hydrogenated because hydrogen is virtually incapable of penetrating to the surface of contact of the metal particle with the carbon filament

phase (on the rear side), though a constant influx of carbon atoms takes place. The frontal (active) part of the metal particle, which catalyses the carbon filament growth, is not screened by carbon for the above-mentioned reasons.

Thus, the addition of hydrogen prevents the deposition of carbon in the form of a film and creates favourable conditions for the formation of carbon filaments.

Nolan *et al.*<sup>139</sup> gave an interesting explanation of the reasons for the formation of carbon deposits of different morphological types. They believe that carbon is accumulated as open forms, *e.g.*, carbon filaments, in the presence of hydrogen. The edge faces of graphite with unsaturated bonds come out, onto the external surface of the filaments, and hydrogen saturates these bonds. In the absence of hydrogen, carbon should be deposited predominantly in such forms as nanotubes or carbon films which do not have any unsaturated bonds on the edge faces. Thus the major products of decomposition of pure CO on highly dispersed nickel particles are carbon films and nanotubes, whereas the hydrogen-diluted CO forms carbon filaments with the coaxial-conical disposition of the graphite planes in the filament body. It is stated that the slope of the graphite cones depends on the hydrogen concentration in the reaction medium. However, in our opinion, Nolan *et al.*<sup>139</sup> give too much attention to the compensation of the energy of the free valences of the edge faces due to the formation of C–H bonds. It is unclear why CO<sub>2</sub> cannot react with carbon atoms and compensate thereby the energy of free valences. Furthermore, it is not taken into account that the neighbouring graphite layers coming onto the external surface of filaments can interact with each other thus closing the free valences.<sup>140</sup> Coming back to the role of hydrogen, let us note that it influences primarily the rate of the filamentous carbon growth, and this, as was shown above, changes the morphology of filaments.

## 10. The formation of carbon filaments at temperatures above 1273 K

The fibres used for the preparation of carbon composite materials are known to be obtained from viscose, polyacrylonitrile, as well as from petroleum or coal pitch. However, these materials have a substantial disadvantage — they are costly. Therefore, the prospect of their replacement by filaments prepared by catalytic methods seems rather attractive. A method for the preparation of carbon fibres from the gas phase [vapour-grown carbon fibres (VGCF)] is being actively developed in the USA, Japan and China.<sup>141–145</sup> To this end, use is made of iron-containing catalysts deposited on ceramic supports or of injection of a benzene solution of ferrocene into a reactor. The sources of carbon are benzene or methane diluted with hydrogen as well as the gaseous waste from the production of coke or from the converter production of steel (CO–CO<sub>2</sub>–H<sub>2</sub>). A useful effect is given by the addition of small amounts of sulfur-containing gases (*e.g.*, H<sub>2</sub>S) to the gas flow of reagents. The reaction is carried out at temperatures 1273–1423 K. The process starts with the catalytic growth of primary fibres, then they become thicker due to the deposition of pyrocarbon. The fibres prepared by the VGCF method have the following characteristics: length, a few millimetres; diameter, 2–3 μm; density, ~ 2 g cm<sup>-3</sup>.

Structural studies showed that the use of iron particles at temperatures above 1173 K can yield long filaments uniform in size, which consist of densely packed cylindrical basal graphite planes and always have a hollow core.

Baird *et al.*<sup>81</sup> have proposed a scheme of the growth of a tubular filamentous carbon which presumes diffusion of small carbon clusters over the surface of a metal particle. This model was further developed in a study of Oberlin *et al.*,<sup>146</sup> which is one of the most detailed investigations of the structure of filamentous carbon formed from a benzene–hydrogen mixture at 1373 K. The reaction products were tubular filaments of cylindrical shape with a hollow channel inside them. The diameter of the channel ranged from 20 to 500 Å and was not always constant along the filament length. In their cross-sections, the filaments had a 'dendritic'

structure: apparently, the graphite layers formed concentric rings. In the core of the filament, the graphite structure was more ordered than in the outer layers. Based on the results obtained, the authors have postulated a two-step mechanism of the filamentous carbon formation. In the first step, the filament core is formed which consists of long parallel carbon layers twisted around the hollow central channel. In the second stage, the filamentous carbon becomes thicker owing to pyrolytic depositions. The ends of filaments contain the catalyst's particles. The interplanar distances measured by the method of electron microdiffraction make it possible to presume that the catalytic particles are either iron carbide (Fe<sub>3</sub>C) or α-Fe. However, no final conclusions have been made.

Tibbetts<sup>147</sup> attempted to establish the reason for the tubular structure of carbon filaments. As the basal face possesses lower specific surface energy than the edge faces, the free energy of the growing filament should be a minimum when the filament consists of curved basal planes forming cylinders. However, as the diameters of cylinders decrease, the degree of curvature of the planes increases and, naturally, the energy required for such curving also increases. Thermodynamic considerations indicate that the formation of a hollow core is more advantageous energetically than the deposition of carbon in the form of strongly deformed cylindrical planes of small diameter. The model proposed made it possible to predict accurately the minimum inner diameter of a carbon filament and to substantiate theoretically the tubular structure of the filamentous carbon.

Deactivation of catalysts at high temperatures is associated with the blockage of the surface of catalytic particles; however, there are different suggestions about the mechanism of this phenomenon. Some investigators believe<sup>93, 147, 148</sup> that deactivation is due to the adsorption, on the frontal side of the metal particle, of highly condensed pyrolysis products, which are formed in the gas phase and are precursors of soot particles. The equation obtained on the basis of this hypothesis provides a satisfactory description of the histogram of the distribution of filaments with respect to their length which are formed upon methane decomposition on γ-Fe at 1320 K. According to Gabelle,<sup>128</sup> the catalyst is active in the liquid state, and even small changes in the surface composition induce its transition to a less active non-melting form which is easily blocked by carbon.

## 11. Growth of carbon filaments under the action of catalytic particles present inside the filament

It was shown that disproportionation of CO on the Fe/Ni and Fe/Co alloys yields the so-called bifilaments.<sup>100</sup> It was established<sup>111, 112</sup> that the growth of bifilaments is catalysed by biconical microcrystals. In their structures, each of the bicones is analogous to a 'simple cone' which initiates the growth of classical filaments. It was established that the directions [100] of the alloy crystal with the body-centred cubic lattice and [110] of the alloy with the face-centred cubic lattice are parallel to the filament axis. In the alloys with the face-centred cubic lattice, the twinning of biconical crystals was often observed. No simple mechanism has yet been proposed for the explanation of the growth of these unusual filaments.

## 12. Regularities and the mechanism of the growth of helical carbon forms

Helical filaments or bifilaments first described by Baker *et al.*<sup>37</sup> were formed on an Fe/Sn alloy from acetylene at temperatures above 1073 K. One catalytic particle of the alloy initiates simultaneous growth of two filaments in the opposite directions. The two corkscrew-like filaments grow with approximately the same velocities, and in the course of the process, identical fragments are reproduced symmetrically in either filament.

Unusual helical forms of filamentous carbon were also observed in the carbonisation of an Ni–Cu/MgO catalyst which was carried out in the medium of buta-1,3-diene diluted with argon and hydrogen in the molar ratio C<sub>4</sub>H<sub>6</sub>:Ar:H<sub>2</sub> = 2:40:75

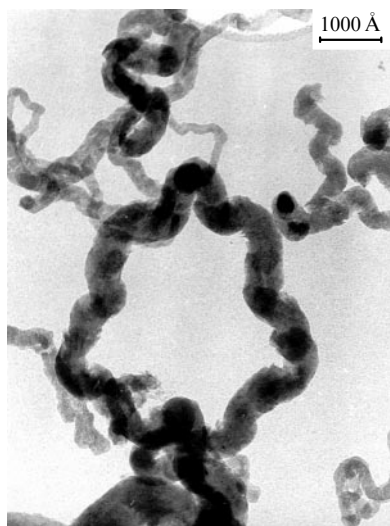


**Figure 13.** A micrograph of the mirror-symmetrical carbon filaments growing from one particle of an Ni–Cu alloy. Due to the increase in the carbon content on the Ni–Cu/MgO catalyst, its mass increased 28-fold (the same refers to Figs 14, 15).

at 723 K.<sup>149</sup> According to the X-ray diffraction data, after the reduction with hydrogen, the Ni–Cu alloy of cubic structure is predominant in the catalyst and the MgO phase is also present.

An electron micrograph of the mirror-symmetrical carbon filaments (Fig. 13) shows that the filaments are twisted into helices and originate from one metal particle. The thickness of these filaments ranges from 300 to 1000 Å, while their lengths reach 1 μm. Obtained by the HREM method, micrographs of metal particles on which carbon grows indicate (Fig. 14) that they possess a nearly symmetrical oval shape with the symmetry planes in the middle part and represent multiple twins. On the frontal side of the surface, in the middle of the oval metal particle there is a

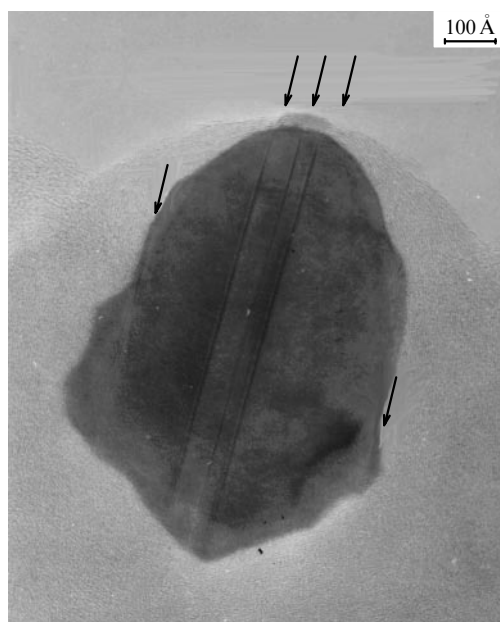


**Figure 14.** A micrograph obtained by the HREM method of an oval particle of an Ni–Cu alloy. The arrows indicate the positions of the twinning boundaries.

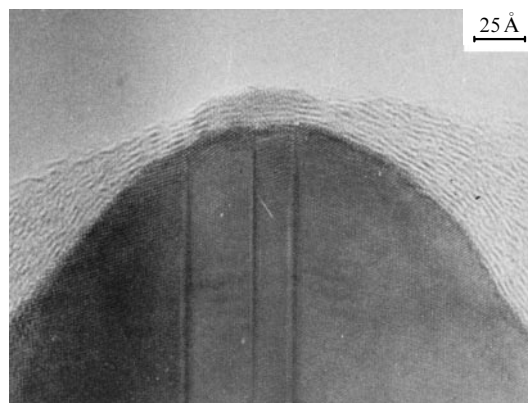


**Figure 15.** A micrograph obtained by the HREM method of the Ni–Cu/MgO catalyst.

microparticle 10–15 Å thick and 30–50 Å wide with the structure of the hexagonal nickel. It is on these microparticles that the ‘chemical’ step of the carbide cycle mechanism is realised.

In the crystalline particles of the Ni–Cu alloy, there is a series of twinning planes (111) which are parallel to the mirror symmetry plane. The twinning planes separate the blocks of twins with the face-centred cubic structure. The interplanar distances in each block of twins are:  $d_{111} = 2.03$  Å and  $d_{002} = 1.7$  Å. In a micrograph obtained by the HREM method, one can easily notice that the twinning planes are grouped under a microphase particle on the frontal side of the crystal (Fig. 15), while they are rarely found in other places. In the catalysts on which the deposition of carbon reaches 2000%–5000%, the widths of twin blocks in a metal usually exceed 20 Å.

At the beginning of the reaction the frequency of the appearance of twins in the metal is much higher than that at its end. In a micrograph of the Ni–Cu/MgO catalyst subjected to carbonisation for 10 min (Fig. 16), one can see the carbonisation boundaries with a period of  $\sim 4$  Å. This distance is sufficient for the placement of only three densely packed layers of atoms of the face-centred cubic lattice of a metal with the interplanar distance  $d_{111} = 2.03$  Å.

The hexagonal nickel carbide  $\text{Ni}_3\text{C}$  (see Ref. 150) and metallic nickel<sup>151</sup> have virtually the same crystal lattices (hexagonal close packing). Carbon atoms in carbide occupy 1/3 of the octahedral cavities in the packing of metal atoms.

According to the mechanism of formation of symmetrical carbon filaments proposed by Zaikovskii *et al.*<sup>149</sup>, in the induction

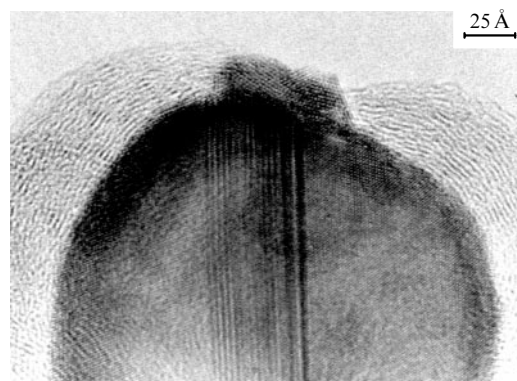


**Figure 16.** A micrograph of the Ni–Cu/MgO catalyst containing 75 mass. % of carbon. In the middle part of the Ni–Cu alloy particle one can see the boundaries of twinning after each 4 Å. The sequence of densely packed layers corresponds to the alternation of the hexagonal and cubic structures of the alloy.

period of the filamentous carbon growth, decomposition of buta-1,3-diene yields a particle of  $\text{Ni}_3\text{C}$  carbide microphase metastable at 723 K, while the Ni–Cu alloy itself is supersaturated with carbon. When critical supersaturation is attained and at some site of the alloy surface a crystalline graphite nucleus is formed, then a rapid ‘discharge’ of carbon atoms onto it occurs. The graphite phase nuclei are preferentially formed on the (111) face of the Ni–Cu alloy since the symmetry and interatomic distances in flat networks (002) of graphite and (111) of the alloy oriented towards the graphite filaments coincide.

Owing to a strong supersaturation of the frontal zone of the metal particle with carbon, an intense diffusion flux of carbon to the places of its crystallisation in the form of graphite phase arises. Rapid diffusion of carbon atoms leads to an enhanced generation of defects in the metal. The metal, while remaining solid, passes to the viscous-fluid state. As a result, the particle of the Ni–Cu alloy acquires spherical shape which is the most advantageous from the energetic viewpoint. However, the diffusive fluxes of carbon atoms also induce dislocation of metal atoms, and the spherical particle is somewhat stretched (Fig. 17). There arises a regime of self-organisation of the symmetrical form of metal particles. As a result, the metal particles acquire an oval form with the symmetry plane in their centre part. In this case, each of the symmetrical halves is oriented in such a manner that the [111] directions of the alloy coincide with the directions of the growth of carbon filaments.

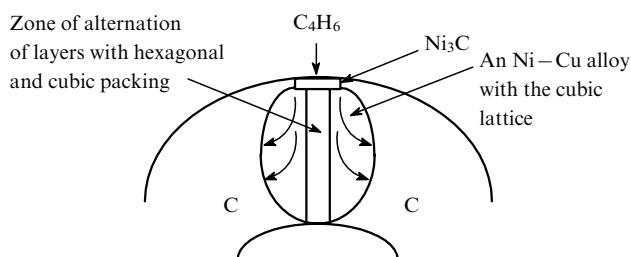


**Figure 17.** The mechanism of the growth of a helical carbon filament obtained from buta-1,3-diene on the Ni–Cu crystals.

A particle of the hexagonal  $\text{Ni}_3\text{C}$  carbide microphase on the frontal side is a nucleus for the growth of a hexagonal structure piercing the catalytic particle of the Ni–Cu alloy. Under the reaction conditions, the catalytic particle consists of alternating layers of cubic and hexagonal Ni–Cu alloys. The passage of carbon atoms through the interlayer of the hexagonal metal may be represented as continuously alternating steps of formation and decomposition of the carbide. However, the saturation of hexagonal interlayers with carbon should decrease as they go farther and farther from the microphase of the hexagonal carbide. Consequently, in the course of reaction the layers of the hexagonal metal include most probably a non-stoichiometric carbide of variable composition.

During the reaction, the twinning planes are dislocated from the central zone of the Ni–Cu alloy to the crystal periphery. The driving forces of the dislocation of the interblock boundaries and, respectively, of restructuring is the diffusion of carbon atoms and the lesser stability of the alloy with the hexagonal structure than that of the alloy with the cubic structure.

Owing to an intense directed flux of carbon atoms from the central part of the crystal to its periphery (see Fig. 17), defects arise in the layers adjoining the twinning planes which induce restructuring of the layers. In other words, the plane of twinning begins to dislocate in the direction of the movement of carbon atoms to the site of carbon crystallisation into the graphite phase. Thus, the hexagonal planar inclusions representing a non-stoichiometric carbide of variable composition ‘disperse’ from the middle of the oval metal–carbon particles. The removal of these

interlayers from the central zone is probably compensated by their repeated regeneration by a microparticle on the surface of a large oval particle in such a way that the process is continuous.

Graphite filaments grow symmetrically and virtually over the entire surface of the Ni–Cu alloy particle. The route of the diffusion of carbon atoms from the place of their entry into the alloy particle through the nickel carbide microphase to different sites of the graphite phase growth is not the same (see Fig. 17). Because of this, the velocities of the graphite phase growth become also different and twisting of filaments occurs to the side opposite to the place where the carbide microparticle is situated.

## IV. Conclusion

The above-discussed observations and conclusions are helpful in understanding the factors that influence the process of carbon filament formation and determine their properties. These properties include primarily the spatial order of the construction of the basal graphite planes in filaments, the diameters and lengths of filaments, the presence or absence of the inner hollow along the axis of filaments, their morphologies, the existence and degree of dispersion of other mineral components in the graphite structure of filaments, *etc.* Adsorption, catalytic, chemical, magnetic, mechanical and many other properties of filaments depend on these characteristics.

Note that the methods for controlling the synthesis of carbon materials are still in their infancy. For this reason, we will touch upon this issue only in brief and in most general terms.

The most substantial effect on the properties of filamentous carbon materials is the spatial distribution of the basal planes of graphite. The distribution of graphite layers in a filament determines such properties of the carbon material as its mechanical strength, adsorption capacity, chemisorption and catalytic characteristics, intercalation capacity and others.

As mentioned above, depending on the properties of the catalytic metal particle (head) and conditions of the implementation of the process, it is possible to synthesise graphite filaments of three major ‘basal’ structural types: with the coaxial-cylindrical, coaxial-conical and stack structures (see Fig. 2). The properties of metal particles which are of interest to us can be regulated by varying the method of their preparation and by adding other metals.

The diameter of a filament is determined by the size of the metal particle and differs little from it. The length of a filament depends on the time of its growth, which in turn is determined by the time during which the metal particle can efficiently play the role of the filament growth centre without undergoing deactivation or breaking into subcrystals.

The regime of the process has a substantial effect on properties of carbon materials not only directly, but also indirectly, through deactivation of metal catalyst particles. A decrease in the temperature of the process, dilution of a hydrocarbon with hydrogen, use of a less coke-producing hydrocarbon will make it possible to increase the yield of carbon formations per unit mass of a metal and to improve the graphite structure. However, in this case, naturally, the rate of carbon formation decreases.

This review was prepared with a financial support of the Russian Foundation for Basic Research (Projects Nos 99-03-32420, 00-03-32431) and the Grant for Leading Scientific Schools of Russian Federation (No. 00-15-97440).

## References

1. R A Buyanov *Kinet. Katal.* **28** 157 (1987)<sup>a</sup>
2. H Storch, N Golubic, R Anderson *The Fischer–Tropsch and Related Syntheses* (New York: Wiley, 1951)
3. Yu B Kagan, A N Bashkurov, S V Kamzolkina, A Ya Rozovskii *Zh. Fiz. Khim.* **23** 2706 (1959)<sup>b</sup>

4. R A Buyanov, V V Chesnokov, A D Afanas'ev, V S Babenko *Kinet. Katal.* **18** 1021 (1977)<sup>a</sup>
5. R A Buyanov *Zakoksovaniye Katalizatorov* (Coking of Catalysts) (Novosibirsk: Nauka, 1983)
6. V V Chesnokov, Candidate Thesis in Chemical Sciences, Institute of Catalysis, Siberian Branch of the Academy of Sciences of the USSR, Novosibirsk, 1982
7. A Ya Rozovskii *Katalizator i Reaktsionnaya Sreda* (Catalyst and Reaction Medium) (Moscow: Nauka, 1988)
8. V V Chesnokov, R A Buyanov, A D Afanas'ev *Kinet. Katal.* **20** 477 (1979)<sup>a</sup>
9. R A Buyanov *Kinet. Katal.* **21** 237 (1980)<sup>a</sup>
10. R A Buyanov, M A Tanatarov, in *Nauchnye Osnovy Tekhnologii Katalizatorov* (Scientific Foundations of the Technology of Catalysts) (Novosibirsk: Institute of Catalysis, Siberian Branch of the Academy of Sciences of the USSR, 1981) No. 13, p. 67
11. R A Buyanov, M A Tanatarov, in *Sbornik Vsesoyuz. Shkoly po Katalizatoram. Lektsii* (Collection of All-Union School on Catalysts. Lectures) (Novosibirsk: Institute of Catalysis, Siberian Branch of the Academy of Sciences of the USSR, 1980) Part 3, p. 4
12. V V Chesnokov, R A Buyanov, A D Afanas'ev, L M Plyasova *Izv. Sib. Otd. Akad. Nauk SSSR. Ser. Khim.* (5) 82 (1980)
13. R A Buyanov, V V Chesnokov, A D Afanas'ev *Izv. Sib. Otd. Akad. Nauk SSSR. Ser. Khim.* (4) 28 (1981)
14. R A Buyanov, V V Chesnokov, A D Afanas'ev *Kinet. Katal.* **20** 207 (1979)<sup>a</sup>
15. V V Chesnokov, R A Buyanov, A D Afanas'ev *Izv. Sib. Otd. Akad. Nauk SSSR. Ser. Khim.* (2) 60 (1982)
16. V V Chesnokov, R A Buyanov, A D Afanas'ev, V S Babenko, in *Kataliticheskaya Konversiya Uglevodorodov* (Catalytic Conversion of Hydrocarbons) (Kiev: Naukova Dumka, 1978) No. 3, p. 38
17. V V Chesnokov, R A Buyanov, in *Proceedings of the Second Indo-Soviet Seminar on Catalysis, Hyderabad, 1986* p. 22
18. V V Chesnokov, R A Buyanov, A D Afanas'ev *Kinet. Katal.* **24** 1251 (1983)<sup>a</sup>
19. V V Chesnokov, R A Buyanov *Kinet. Katal.* **28** 403 (1987)<sup>a</sup>
20. I Stensgaard, L Ruan, E Laegsgaard, F Besenbacher *Surf. Sci.* **337** 190 (1995)
21. W Huber, M Weinelt, P Zebisch, H-P Steinruck *Surf. Sci.* **253** 72 (1991)
22. D R Huntley, S L Jordan, F A Grimm *J. Phys. Chem.* **96** 1409 (1992)
23. Yu D Tret'yakov *Tverdofaznye Reaktsii* (Solid-Phase Reactions) (Moscow: Khimiya, 1978)
24. E V Khamskii *Kristallizatsiya iz Rastvorov* (Crystallisation from Solutions) (Leningrad: Nauka, 1967)
25. V V Chesnokov, Doctoral Thesis in Chemical Sciences, Institute of Catalysis, Siberian Branch of the Russian Academy of Sciences, Novosibirsk, 1999
26. A K Damask, K D Khoman *Diffuziya v Metallakh s Ob'emno-tsentrirovannoi Reshetkoi* (Diffusion in Metals with Body-Centred Lattice) (Moscow: Metallurgiya, 1969)
27. R T K Baker, P S Harris, in *Chemistry and Physics of Carbon* (Eds P L Walker Jr, P A Thrower) (New York: Marsel Dekker, 1978) p. 83
28. Y Miura, T Uchijima, S Makishima *J. Chem. Soc. Jpn., Ind. Chem. Soc.* **71** 86 (1968)
29. V V Veselov, P S Pilipenko *Kinet. Katal.* **11** 1590 (1970)<sup>a</sup>
30. P S Pilipenko, V V Veselov *Poroshk. Metall.* **9** 150 (1975)
31. V V Veselov, Doctoral Thesis in Chemical Sciences, L V Pizarzhevskii Institute of Physical Chemistry, Academy of Sciences of the Ukrainian SSR, Kiev, 1975
32. V V Veselov, P S Pilipenko, in *Kataliticheskaya Konversiya Uglevodorodov* (Catalytic Conversion of Hydrocarbons) (Kiev: Naukova Dumka, 1975) No. 2, p. 35
33. R T K Baker, M A Barber, P S Harris, F S Feates, R J Waite *J. Catal.* **26** 51 (1972)
34. S A Bernardo, L S Lobo *J. Catal.* **37** 267 (1975)
35. R T K Baker, P S Harris, R B Thomas, R J Waite *J. Catal.* **30** 86 (1973)
36. R T K Baker, R J Waite *J. Catal.* **37** 101 (1975)
37. R T K Baker, P S Harris, S Terry *Nature (London)* **253** 37 (1975)
38. R T K Baker, G R Gadsby, R B Thomas, R J Waite *Carbon* **13** 211 (1975)
39. R T K Baker, P S Harris, H J Henderson, R B Thomas *Carbon* **13** 17 (1975)
40. S D Gertsriken, I Ya Dekhtyar *Diffuziya v Metallakh i Splavakh v Tverdoi Faze* (Diffusion in Metals and Alloys in the Solid Phase) (Moscow: Fizmatgiz, 1960)
41. P L Gruzin, Yu A Polikanov, T B Fedorov *Fiz. Met. Metalloved* **4** 94 (1975)
42. W Seith, T Heumann *Diffusion in Metallen* (Berlin: Springer, 1955)
43. J D Fast *Interaction of Metals and Gases* Vol. 2 (London: Macmillan, 1971)
44. I I Kovenskii *Fiz. Met. Metalloved.* **16** 613 (1963)
45. V K Kh Krol', P Delizhyur, K Mirodatos *Kinet. Katal.* **37** 698 (1996)<sup>a</sup>
46. M B Lee, Q Y Yang, S L Tang, S T Ceyer *J. Chem. Phys.* **85** 1693 (1986)
47. M B Lee, Q Y Yang, S T Ceyer *J. Chem. Phys.* **87** 2724 (1987)
48. J D Beckerle, Q Y Yang, A D Johnson, S T Ceyer *J. Chem. Phys.* **86** 7236 (1987)
49. S T Ceyer, J D Beckerle, M B Lee, S L Tang, Q Y Tang, M A Hines *J. Vac. Sci. Technol. A, Vac. Surf. Films* **5** 501 (1987)
50. A V Hamza, R J Madix *Surf. Sci.* **179** 25 (1987)
51. T P Beebe, D W Goodman, B D Kay, J T Yates Jr *J. Chem. Phys.* **87** 2305 (1987)
52. A G Sault, D W Goodman *J. Chem. Phys.* **88** 7232 (1988)
53. X Jiang, D W Goodman *Catal. Lett.* **4** 173 (1990)
54. I Chorkendorff, I Alstrup, S Ullmann *Surf. Sci.* **227** 291 (1990)
55. L Hanley, Z Xu, J T Yates *Surf. Sci. Lett.* **248** L265 (1991)
56. F C Schouten, E W Kaleveld, G A Bootsma *Surf. Sci.* **63** 460 (1977)
57. I Alstrup, M T Tavares *J. Catal.* **135** 155 (1992)
58. M C Demicheli, E N Pouzi, A O Ferretti, A A Yerman *J. Chem. Eng.* **46** 129 (1991)
59. I Alstrup, M T Tavares *J. Catal.* **139** 524 (1993)
60. H J Grabke *Ber. Bunsenges. Phys. Chem.* **69** 409 (1965)
61. H J Grabke *Metall. Trans.* **1** 2972 (1970)
62. J-W Snoeck, G F Froment, M Fowles *J. Catal.* **169** 250 (1997)
63. V V Chesnokov, V I Zaikovskii, R A Buyanov, V V Molchanov, L M Plyasova *Kinet. Katal.* **35** 146 (1994)<sup>a</sup>
64. E R Gilliland, P Harriott *Ind. Chem. Eng.* **46** 10 (1954)
65. G G Kuvshinov, Yu I Mogilykh, D G Kuvshinov *Catal. Today* **42** 357 (1998)
66. P S Pilipenko, V V Veselov, in *Kataliticheskaya Konversiya Uglevodorodov* (Catalytic Conversion of Hydrocarbons) (Kiev: Naukova Dumka, 1978) No. 3, p. 33
67. E G M Kuijper, J W Jansen, A J van Dillen, J W Gent *J. Catal.* **72** 75 (1981)
68. R A Campbell, J S Lenz, D W Goodman *Catal. Lett.* **17** 39 (1993)
69. V B Felonov *Poristy Uglerod* (Porous Carbon) (Novosibirsk: Institute of Catalysis of Russian Academy of Sciences, 1995)
70. S Iijima *Nature (London)* **354** 56 (1991)
71. M Jose-Vacaman, M Miki-Yoshida, I Rendon, J G Santiesteban *Appl. Phys. Lett.* **62** 657 (1993)
72. P E Nolan, A H Cutler, D C Lynch, in *Engineering, Construction, and Operations in Space IV* (Eds R G Galloway, S Lokaj) (New York: American Society of Civil Engineers, 1994) Vol. 2, p. 1199
73. P Chen, H-B Zhang, G-D Lin, Q Hong, K R Tsai *Carbon* **35** 1495 (1997)
74. T W Ebbesen, P M Ajayan *Nature (London)* **358** 220 (1992)
75. C McKee *Appl. Catal. A* **98** N2 (1993)
76. L S K Pang, J D Saxby, S P Chattfield *J. Phys. Chem.* **97** 6941 (1993)
77. V I Zaikovskii, V V Chesnokov, R A Buyanov *Appl. Catal.* **38** 41 (1988)
78. R A Buyanov, V V Chesnokov *Zh. Prikl. Khim.* **70** 978 (1997)<sup>c</sup>
79. R A Buyanov, V V Chesnokov *Khim. Inter. Ustoich. Razv.* **3** 177 (1995)
80. N A Prokudina, V V Chesnokov, N A Zaitseva, L M Plyasova, V I Zaikovskii, A V Golovin, V Yu Gavrilov *Sib. Khim. Zh.* (3) 122 (1991)
81. T Baird, J R Fryer, B Grant *Carbon* **12** 591 (1974)
82. J R Rostrup-Nielsen *Catalysis, Science and Technology* (Eds J R Anderson, M Boudart) (Berlin: Springer, 1984) Vol. 5, p. 1
83. F J Derbyshire, D L Trimm *Carbon* **13** 189 (1975)
84. S D Robertson *Carbon* **8** 365 (1970)
85. E L Evans, J M Thomas, P A Thrower, P L Walker *Carbon* **11** 441 (1973)
86. C W Keep, R T K Baker, J A France *J. Catal.* **47** 232 (1977)
87. J R Rostrup-Nielsen *J. Catal.* **27** 343 (1972)

88. T Wada, H Wada, J F Elliott, J Chipman *Metall. Trans.* **2** 2199 (1971)
89. R T K Baker, J J Chludzinski Jr *J. Catal.* **64** 464 (1980)
90. L S Lobo, D L Trimm *J. Catal.* **29** 15 (1973)
91. J L Figueiredo, D L Trimm *J. Appl. Chem. Biotechnol.* **28** 611 (1978)
92. S D Robertson *Nature (London)* **221** 1044 (1969)
93. G G Tibbetts, M G Devour, E J Rodda *Carbon* **25** 367 (1987)
94. R T Yang, J P Chen *J. Catal.* **115** 52 (1989)
95. R T Yang, K L Yang *J. Catal.* **90** 194 (1984)
96. R T Yang, K L Yang *J. Catal.* **93** 182 (1985)
97. J R Rostrup-Nielsen, D L Trimm *J. Catal.* **48** 155 (1977)
98. M Audier, M Coulon, L Bonnetain *Carbon* **21** 93 (1983)
99. M Audier, M Coulon, L Bonnetain *Carbon* **21** 105 (1983)
100. M Audier, M Coulon, L Bonnetain *Carbon* **21** 99 (1983)
101. A Sacco Jr, P Thacker, T N Chang, A T S Chiang *J. Catal.* **85** 224 (1984)
102. A Sacco Jr, P Thacker, in *Proceedings of the 16th Biennial Conference on Carbon, San Diego, CA 1983* p. 525
103. P K DeBokx, A J H M Kock, E Boellaard, W Klop, J W Geus *J. Catal.* **96** 454 (1985)
104. A J H M Kock, P K DeBokx, E Boellaard, W Klop, J W Geus *J. Catal.* **96** 468 (1985)
105. E Boellaard, P K DeBokx, A J H M Kock, J W Geus *J. Catal.* **96** 481 (1985)
106. I Alstrup *J. Catal.* **109** 241 (1988)
107. E C Bianchini, C R F Lund *J. Catal.* **117** 455 (1989)
108. G G Kuvshinov, S G Zavarukhin, Yu I Mogil'nykh, D G Kuvshinov *Khim. Promst* **5** 48 (1998)
109. M Audier, M Coulon *Carbon* **23** 317 (1985)
110. M Audier, A Oberlin, M Oberlin, M Coulon, L Bonnetain *Carbon* **19** 217 (1981)
111. M Audier, A Oberlin, M Coulon *J. Cryst. Growth* **55** 549 (1981)
112. M Audier, A Oberlin, M Coulon *J. Cryst. Growth* **57** 524 (1982)
113. M Audier, M Coulon, A Oberlin *Carbon* **18** 73 (1980)
114. M Audier, J P Simon, P Guyot *Acta Metall.* **34** 1982 (1986)
115. M Audier, P Bowen, W Jones *J. Cryst. Growth* **63** 125 (1983)
116. L Bonnetain, P Gabelle, M Audier, in *Carbon Fibres, Filaments and Composites (NATO ASI, Ser. C, Math. Phys. Sci.)* (Eds J L Figueiredo, C A Bernardo, R T K Baker, K J Huttinger) (Dordrecht: Kluwer Academic, 1990) Vol. 177, p. 507
117. N M Rodriguez, A Chambers, R T K Baker *Langmuir* **11** 3862 (1995)
118. F C Schouten, O L J Gijzeman, G A Bootsma *Surf. Sci.* **87** 1 (1979)
119. F C Schouten, O L J Gijzeman, G A Bootsma *Bull. Soc. Chim. Belg.* **88** 541 (1979)
120. G A Somorjai *Surf. Sci.* **242** 481 (1991)
121. M Eizenberg, J M Blakely *Surf. Sci.* **82** 228 (1979)
122. R A Buyanov, V V Chesnokov *Khim. Inter. Ustoich. Razv.* **5** 619 (1997)<sup>d</sup>
123. V V Chesnokov, R A Buyanov, A D Afanas'ev *Kinet. Katal.* **25** 1152 (1984)<sup>a</sup>
124. L B Avdeeva, O V Goncharova, D I Kochubey, V I Zaikovskii, L M Plyasova, B N Novgorodov, Sh K Shaikhutdinov *Appl. Catal. A* **141** 117 (1996)
125. V N Parmon *Catal. Lett.* **42** 195 (1996)
126. R S Wagner, W C Ellis *Trans. AIME* **233** 1053 (1965)
127. F Benissad, P Gabelle, M Coulon, L Bonnetain *Carbon* **26** 425 (1988)
128. P Gabelle, in *Carbon Fibres, Filaments and Composites (NATO ASI, Ser. C, Math. Phys. Sci.)* (Eds J L Figueiredo, C A Bernardo, R T K Baker, K J Huttinger) (Dordrecht: Kluwer Academic, 1990) Vol. 177, p. 95
129. G G Tibbetts, E J Rodda *Mater Res. Soc. Symp. Proc.* **111** 49 (1988)
130. G G Tibbetts, M P Balogh, in *The 23rd Biennial Conference on Carbon (Expanded Abstracts and Program) Pennstate Campus, 1997* Vol. 2, p. 288
131. H P Boehm *Carbon* **11** 583 (1973)
132. M P Manning, R C Reid *Ind. Eng. Chem., Proc. Des. Dev.* **16** 358 (1977)
133. V V Chesnokov, V I Zaikovskii, R A Buyanov, V V Molchanov, L M Plyasova *Catal. Today* **24** 265 (1995)
134. C A Bernardo, I Alstrup, J R Rostrup-Nielsen *J. Catal.* **96** 517 (1985)
135. P C M van Stiphout, D E Stoble, F Th V D Scheur, J W Geus *Appl. Catal.* **40** 219 (1988)
136. R A Buyanov, A D Afanas'ev, V V Chesnokov *Kinet. Katal.* **19** 1072 (1978)<sup>a</sup>
137. D A Wesner, F P Coenen, H P Bonzel, in *The Structure of Surfaces II* (Eds J F van der Veen, M A Van Hove) (Berlin: Springer, 1988) Vol. 11, p. 612
138. R A Buyanov, A D Afanas'ev, V V Chesnokov, V S Babenko, in *Geterogennyi Kataliz (Tr. IV Mezhdunarod. Simp.)* [Heterogeneous Catalysis (Proceedings of the IVth International Symposium)] (Varna: Bulgarian Academy of Sciences, Centre on Chemistry, 1979) Part 1, p. 355
139. P E Nolan, M J Schabel, D C Lynch, A H Cutler *Carbon* **33** 79 (1995)
140. Sh K Shaikhutdinov, V I Zaikovskii, L B Avdeeva *Appl. Catal. A* **148** 123 (1996)
141. G G Tibbetts *J. Cryst. Growth* **73** 431 (1985)
142. M Ishioka, T Okada, K Matsubara, M Endo *Carbon* **30** 859 (1992)
143. M Ishioka, T Okada, K Matsubara, M Endo *Carbon* **30** 865 (1992)
144. M Ishioka, T Okada, K Matsubara *Carbon* **30** 975 (1992)
145. T Kato, K Haruta, K Kusakabe, S Morooka *Carbon* **30** 989 (1992)
146. A Oberlin, M Endo, T Kayama *J. Cryst. Growth* **32** 335 (1976)
147. G G Tibbetts *J. Cryst. Growth* **66** 632 (1984).
148. G G Tibbetts, in *Carbon Fibres, Filaments and Composites (NATO ASI, Ser. C, Math. Phys. Sci.)* (Eds J L Figueiredo, C A Bernardo, R T K Baker, K J Huttinger) (Dordrecht: Kluwer Academic, 1990) Vol. 177, p. 73
149. V I Zaikovskii, V V Chesnokov, R A Buyanov *Kinet. Katal.* **40** 612 (1999)<sup>a</sup>
150. S Nagakura *J. Phys. Soc. Jpn.* **12** 482 (1957)
151. G Carturan, G Cocco, S Enzo, R Gauzerla, M Jenarda *Mater. Lett.* **7** 47 (1988)

<sup>a</sup> — *Kinet. Catal. (Engl. Transl.)*

<sup>b</sup> — *Russ. J. Phys. Chem. (Engl. Transl.)*

<sup>c</sup> — *Russ. J. Appl. Chem. (Engl. Transl.)*

<sup>d</sup> — *Chem. Sustainable Dev. (Engl. Transl.)*